

Finite Orbits in Multivalued Maps and Bernoulli Convolutions

Christoph Bandt and Rüdiger Zeller *

October 24, 2016

Abstract

Bernoulli convolutions form a parametric family of measures generated by multivalued maps from a real interval onto itself. In spite of their simple definition, they are still not well understood. We suggest to study their two-dimensional density which exists by a theorem of Solomyak, and the finite orbits of the multivalued maps.

Outside the overlapping region, there are ordinary periodic and preperiodic orbits, studied by Erdős, Jón, Komornik, Sidorov, de Vries and others as points with unique addresses, and by Jordan, Shmerkin and Solomyak as points with maximal local dimension. These orbits form address curves related to the Milnor-Thurston itineraries in one-dimensional dynamics. The curves depend smoothly on the parameter and represent quantiles of all corresponding Bernoulli convolutions.

Inside the overlap region, address curves can intersect and give rise to network-like orbits. This can happen only at Perron parameters. Intersection points can have finite or countable number of addresses, as found by Sidorov. For an uncountable number of parameters, the midpoint of the interval has only two addresses. The intersection of periodic address curves, however, can lead to singularities of the measures. We give examples which are not Pisot or Salem parameters.

It seems that all singularities of Bernoulli convolutions are related to network-like orbits. The paper is self-contained and includes many illustrations.

1 Introduction

This paper studies two related subjects: the occurrence of network-like orbits in multivalued maps, and the parametric family of Bernoulli convolutions, BCs for short. The orbit of a point x in a dynamical system can be visualized as a path of arrows leading from $f^k(x)$ to $f^{k+1}(x)$ for $k = 0, 1, 2, \dots$. The orbit becomes finite if x fulfils the equation $f^{k+p}(x) = f^k(x)$ for some k and p , so that the path turns into a cycle. For a multivalued map, the orbit of x is represented by a branching tree. Such orbit can only be finite if all branches lead back to lower levels of the tree, which is usually expressed by several equations, determining not only the point x but also the mapping f , at least to some extent. Nevertheless, network-like orbits appear in simple multivalued maps of an interval, in particular those which define BCs.

Bernoulli convolutions are the simplest examples of self-similar measures with overlaps, and have been studied as examples in real analysis since the 1930s. Given a number β between 1 and 2, let $t = 1/\beta$ and consider the two linear functions

$$g_0 : [0, t] \rightarrow [0, 1], \quad g_0(x) = \beta x \quad \text{and} \quad g_1 : [1 - t, 1] \rightarrow [0, 1], \quad g_1(x) = \beta x + 1 - \beta,$$

as indicated in Figure 1. The BC with parameter β is the unique probability measure ν on $[0, 1]$ which fulfils

*This work was supported by Deutsche Forschungsgemeinschaft grant Ba 1332/11-1.

$$\nu(A) = \frac{1}{2}\nu(g_0(A)) + \frac{1}{2}\nu(g_1(A)) \quad \text{for all Borel sets } A \subset [0, 1]. \quad (1)$$

When A is a subset of $[0, 1-t]$ or $[t, 1]$, only one term will appear on the right of (1) since $g_1(A)$ or $g_0(A)$ is empty. The map $G(x) = \{g_0(x), g_1(x)\}$ is multivalued only for $x \in [1-t, t]$, the so-called overlap region. Basic facts on BCs can be found in [47, 39, 8] and in Section 6. Definitions of Pisot and Garsia numbers are given in Section 4.

Since Erdős [15] proved in 1939 that BCs for Pisot numbers β are singular measures, much work was done to determine those β for which ν is absolutely continuous. There are detailed studies of BCs of Pisot numbers [4, 18, 20, 33, 25] and other algebraic numbers [22, 21, 19, 50]. Singularity of ν is still only known for the countable set of Pisot numbers, and regularity of specific Bernoulli convolutions could be shown only for the countable set of Garsia numbers [22], not even for any particular rational number β . However, Solomyak [46] proved in 1995 that for Lebesgue almost all β the measure ν has a density function, even an L^2 density function as shown by Peres and Solomyak [38]. In other words, if we take a random number β between 1 and 2, then ν will have a density function with probability one. See the surveys [39, 47] for more information on a lot of related work. Recently, Shmerkin [41] used new tools of Hochman to improve Solomyak's result further: the set of β leading to singular BCs has Hausdorff dimension zero. Very recently, Varju [50] proved that for all algebraic numbers $\beta \in [2 - \varepsilon, 2]$ fulfilling a technical condition, the measure ν is absolutely continuous. However, ε was not specified, it could be as small as $10^{-10^{10}}$.

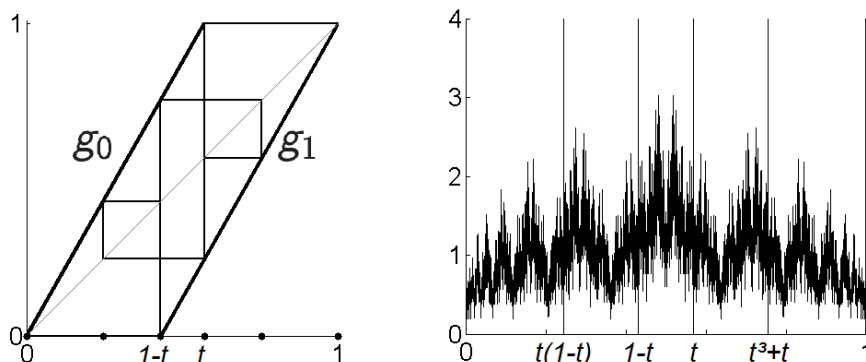


Figure 1: The mappings $g_0(x) = \beta x$, $g_1(x) = \beta x + 1 - \beta$ and the corresponding Bernoulli convolution for $\beta \approx 1.7549$. Actually, β is a Pisot number with polynomial $\beta^3 - 2\beta^2 + \beta - 1$. So $t = 1/\beta$ has a finite orbit which is indicated here, together with the generated partition.

This paper follows a different path. We try to study ν for the interesting parameter region $\beta \in [1.01, 1.99]$ and include structural properties of ν studied by Erdős, J6o, Komornik, Sidorov, de Vries and others [16, 23, 14, 29, 33, 43, 44] in connection with β -expansions. We consider all ν_t with $t = 1/\beta \in (\frac{1}{2}, 1)$ together as a two-dimensional 'super-measure'. Solomyak's work implies that this measure is given by an L^2 density function of two variables. The problem to classify BCs into 'singular' and 'regular' now turns into the study of singularities of an L_2 function on a rectangle.

Theorem 1 (Two-dimensional density of Bernoulli convolutions [46, 38])

There is an L^2 function $\Phi : [\frac{1}{2}, 1] \times [0, 1] \rightarrow [0, \infty)$ such that for Lebesgue almost all parameters $t = 1/\beta \in [\frac{1}{2}, 1]$, the density of the Bernoulli convolution ν_t is the function $\Phi(t, x)$, $x \in [0, 1]$.

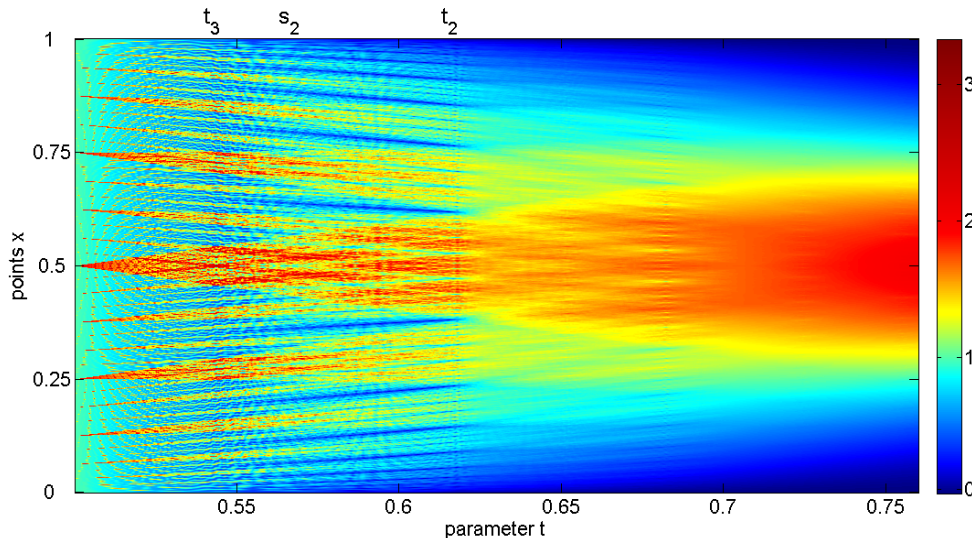


Figure 2: The function Φ for $0.5 \leq t \leq 0.76$. Bernoulli convolutions for 4000 values $t = 1/\beta$ were approximated by histograms, and visualized as vertical sections over t with color code indicated on the right. The measure of Figure 1 appears at $t = s_2 \approx 0.57$. The average value is 1. The overlap region $\mathbf{D} = \{(t, y) \mid t \leq y \leq 1 - t\}$ contains large values.

Figure 2 shows an approximation of Φ for $0.5 \leq t \leq 0.76$. The intricate structure in this picture will be studied in Sections 6-10 where magnifications of Figure 2 are shown. The small values of Φ , drawn in dark blue, as well as the large values, drawn in red, follow certain patterns. The purpose of our paper is to clarify this structure, and see whether it helps to understand the singularity of certain Bernoulli convolutions, and the way how the measures ν_t change with the parameter t .

In the middle of Figure 2 we see the triangular overlap region $\mathbf{D} = \{(t, y) \mid t \leq y \leq 1 - t\}$ which contains large values of Φ . In Section 6 we explain the smaller overlap regions which form 'horns' with tip on the left axis. Next, there is a kind of phase transition at the Fibonacci parameter $t_2 \approx 0.618$. On the left of t_2 , dark blue curves separate the horns. Henceforth, we focus on this case $t < t_2$ where we have apparent structure. The dark curves outside \mathbf{D} become more numerous when t goes down to $\frac{1}{2}$, and they seem to form a Cantor structure. Actually, they consist of points with unique address in the fractal construction, so we have $\Phi(t, y(t)) = 0$ for almost all t on such a curve $y(t)$, which accounts for their color.

The intersection set A_t of the dark curves with the vertical line at t is a well-studied object: the set of points with a unique address for ν_t , and for β -expansion. Around 1990, Erdős and co-authors started to consider the set of univoque numbers, which in Figure 2 appears as the set of parameters t where the dark curves enter the overlap triangle \mathbf{D} , see Proposition 12. It was proved that A_t is infinite for $t < t_2$, see [16] and its references, and Daroczy and Katai [13, 12]. Komornik and Loreti [33] found the constant $\beta_{KL} \approx 1.7872$ at which A_t becomes uncountable. Allouche and Cosnard [3] proved that this constant is transcendental. Glendinning and Sidorov [23] defined the set A_t , proved that it contains accumulation points for $t \leq s_2 \approx 0.57$ and is a Cantor set for $\frac{1}{2} < t < t_{KL}$. Further work includes [2, 4, 42, 43, 44, 30, 29, 32] and the comprehensive paper of de Vries and Komornik [14] on the topology of A_t and of the set of univoque numbers.

In Section 7 and 8, we provide a self-contained approach to all these results. While the

quoted authors used β -expansions, we define binary itineraries and address curves, similar to the technique introduced by Milnor and Thurston [36] for the study of unimodal maps. In our view, A_t is the set on which $G(x) = \{g_0(x), g_1(x)\}$ acts as an ordinary map. Our basic Proposition 8 says that the action of G on A_t is conjugate to the doubling map $g(x) = 2x \bmod 1$ on a corresponding subset of $[0, 1]$, for all $t < t_2$.

The turn from Cantor sets $A_t \subset [0, 1]$ to address curves $y_b(t)$ for binary sequences b in the two-dimensional setting is a new aspect. These curves form a smooth element in an otherwise chaotic scenario. In Theorem 9 we show that each address curve $y_b(t)$ describes the b -quantile of all BCs in its domain. Here b is considered as binary number in $[0, 1]$. All ordinary periodic and preperiodic points of the map G are represented by address curves, and the parameters where such curves enter \mathbf{D} are landmarks of Φ .

Although Φ describes just a measure on a rectangle, we consider it as a representation of a parametric family of dynamical systems, like the Mandelbrot set, or the bifurcation diagram of the family of real quadratic maps [11, 37]. Our approach with binary itineraries underlines the tight connection between these three objects which are all based on the doubling map $g(x) = 2x \bmod 1$. Allouche, Clarke and Sidorov [2] verified the Sharkovskii order for periodic points in A_t . In Section 8 we show that unimodal maps and the sets A_t are in a one-to-one correspondence provided by binary itineraries, which allows to transfer other results between the two theories.

Thus the dynamics of G is well understood on the sets A_t where it is an ordinary map. The difficulty comes when we go inside the overlap region where G is really multivalued. However, we can extend the address curves into \mathbf{D} and consider their intersections. If at least one of the addresses is nonperiodic and the G -orbit of the intersection point y does not return to the overlap interval, then y has either two or a countable number of addresses (Propositions 16 and 19). This implies that the local dimension of ν_t at y assumes the same maximum as at the points with unique addresses. Such points were studied by Sidorov [44], see also [6, 7]. In Section 9, we discuss this case, solve a problem of [44] and prove the following surprising fact (Theorem 18): for an uncountable number of parameters, the central point $\frac{1}{2}$ has only two addresses.

The intersection of address curves is most interesting when both addresses are periodic. This case, discussed in Section 10, is the only one which can lead to singularities of Φ . Here the G -orbit returns to D through at least two different cycles, and we can estimate the local dimension of $d = d_y(\nu)$ at the intersection point y . In the supercritical case where $d > 2t$ there is a singularity, which means that ν cannot have a bounded or continuous density function (Theorem 21). This includes a theorem of Feng and Wang [21]. We provide new examples of parameters with such weak singularities which are neither Pisot nor Salem. One of them is shown in Figure 3: the Perron number $\beta \approx 1.6851$ has higher peaks than nearby Pisot parameters but probably the corresponding BC has an L_1 density.

There are many 'subcritical' intersections of periodic address curves where we expect a bounded density of ν and a nontrivial multifractal spectrum, as found by Feng [19] and Jordan, Shmerkin and Solomyak [29]. Moreover, Theorem 7 says that intersections of periodic or preperiodic address curves can happen only for parameters β which are weak Perron numbers. In his last paper, Thurston [48] pointed out the importance of weak Perron numbers in one-dimensional dynamics.

The illustrations in this paper required a lot of work. The 'chaos game', used in [47, 5] and for Figure 1, is not sufficiently accurate. For the other figures, a Markov chain model was used, where $[0, 1]$ was divided into n intervals of equal length, with $4 \cdot 10^3 \leq n \leq 4 \cdot 10^6$. For large magnifications, inverse iteration can be used, that is, we can directly count the

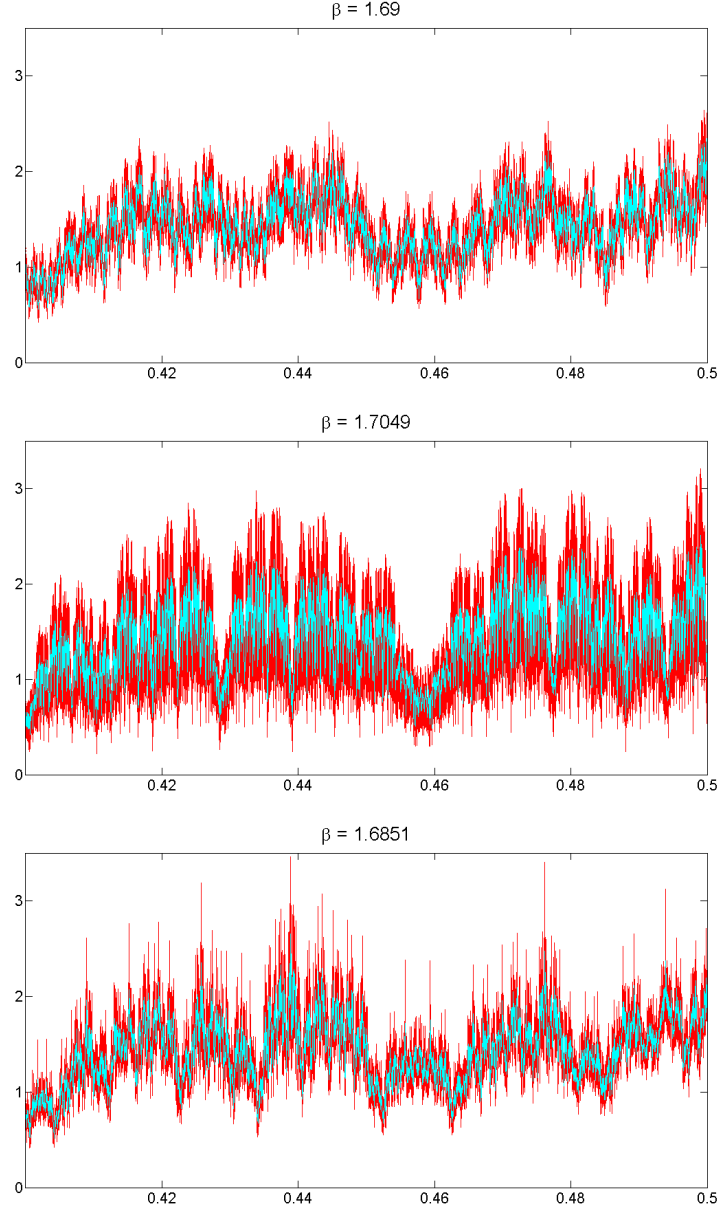


Figure 3: An impression of Bernoulli convolutions for parameters $\beta = 1.69$ (presumably a density function, even continuous), $\beta \approx 1.7049$ (Pisot parameter, singular measure) and $\beta = 1.6851$ (Perron parameter, see Section 10). The Matlab figures include 5000 blue and 250000 red equidistant points in $[0.4, 0.5]$, adjacent values are connected by lines.

offspring of points x under the iteration of G , as given in Definition 1 below. The drawback of that method is the increase of rounding errors under iteration of expanding maps. We do not discuss numerical methods here since they serve for illustration only.

Nevertheless, our opinion is that computer experiments and explicit approximation of fractal measures are appropriate tools for developing intuition and fostering communication. Bernoulli convolutions are a good testbed for fractal measures: on one hand they include

a wide variety of examples, see [8, Section 2], and on the other hand they are 'pure Type' [39, Section 3] and have the same properties on each subinterval of $[0, 1]$, due to their self-similar construction. Let us mention that some types of everyday 'big data' come as fractal measures with several millions of bins: measurements of workload of a server, river discharges, precipitation, particulate matter, activity on financial markets. Singularities, that means extreme values, are of paramount importance in all these fields.

The intuition given by Figure 3 is as follows. The upper function shows the typical BC, the appearance which by Solomyak holds for almost every β . The function is probably continuous, but fractal. It shows more, but finer detail on higher resolution, like Weierstrass functions or Brownian motion. This could be made precise by determining a Hölder exponent or a dimension of the graph. For $\beta \rightarrow 2$ or $t \rightarrow \frac{1}{2}$ we can expect that the Hölder exponent goes to zero and the dimension to 2. This increasing roughness is the most obvious trend which can be seen in BCs, see [8, Section 2]. It was predicted from the convolution structure already by Erdős and others in the 1930s.

The middle panel of Figure 3 shows a singular measure, not a function. This is a typical BC of a Pisot number. The variation of the approximating function is large, increased detail on higher resolution does not become finer, and values tend both to zero and infinity, yet not as fast as one could expect. The lower function represents a Perron parameter which is discussed in Section 10. This is a nowhere continuous function, with a dense set of poles, as we will show. The peaks of the function are higher than those of the comparable Pisot parameter, nevertheless the impression is that it is less singular than the Pisot BC. We do not know whether this BC is a singular measure, but we would guess that it is rather an L_1 -function. Thus there are certain Perron parameters which lead to a lower degree of singularity than Pisot numbers.

We have two conjectures. First, ν has a bounded density unless β is weak Perron. This would imply that only countably many BCs are singular, and all rational parameters lead to bounded densities. Already Garsia [22] made a similar conjecture, and most colleagues will probably agree. The second conjecture, supported by our computer experiments, sounds more unlikely: the parameters t for which ν_t is singular are nowhere dense. It could be even possible that Φ is continuous outside a nowhere dense set of parameters.

We tried hard to make our presentation self-contained, lucid, and comprehensible to a wider audience. The following Sections 2 and 3 contain basic concepts and facts. We introduce our type of multivalued map and the important properties of finite orbits. In Section 4 we give examples of network-like orbits for the Fibonacci BC. In Theorem 6 an infinite family of irreducible orbits of this type are constructed. In Section 5 we prove that network-like orbits in the BC family are only possible for weak Perron parameters. Section 6 introduces the fractal construction of BCs and of the function Φ . In Sections 7 and 8, we define address curves and discuss points with unique addresses. Section 9 and 10 deal with the intersections of address curves inside the overlap region.

2 Some definitions

We consider multivalued maps on real intervals which consist of a finite number of branch maps, as in [28]. We start with a general setting and then focus on more particular cases.

Definition 1 (Branching dynamical system)

A branching dynamical system on $[a, b] \subset \mathbb{R}$ is given by a set of subintervals $I_i \subset [a, b]$ and continuous mappings $g_i : I_i \rightarrow [a, b]$, $i = 1, \dots, m$.

For each point $x \in [a, b]$, the set of immediate successors is $G(x) = G^1(x) = \{g_i(x) \mid x \in I_i\}$. The successors of q^{th} generation are given by the recursion $G^q(x) = G(G^{q-1}(x))$. The orbit of x is $O(x) = \bigcup_{q=0}^{\infty} G^q(x)$ with $G^0(x) = \{x\}$.

The orbits of a branching dynamical system have the structure of a rooted infinite tree, with 0 up to m immediate successors for each vertex. If some values in the orbit coincide, the tree structure is modified and cycles appear. Here we are interested in the case that various successors coincide and the tree becomes a finite network.

An interesting problem for branching dynamical systems is the existence of an absolutely continuous invariant measure μ with a corresponding growth factor λ in the sense that

$$\lambda \cdot \mu(A) = \sum_{i=1}^m \mu(g_i^{-1}(A)) \quad \text{for Borel sets } A \subset [a, b].$$

Next, one can ask for ergodic theorems, which involves the question of asymptotic independence of successors on disjoint branches of the orbit of x . One may also ask for the growth factor λ_x of the number of successors for different x , and its connection with λ , see [20, 31] and Section 3. It would be very interesting to know under which conditions the $G^q(x)$ approach an asymptotic distribution for $q \rightarrow \infty$. These problems are difficult, so we consider more special systems. For ordinary dynamical systems, the first condition below was formulated in [35] to show the existence of an invariant measure μ .

Definition 2 (Fractal and linear branching systems)

A branching dynamical system $\{g_i : I_i \rightarrow [a, b], i = 1, \dots, m\}$ is called fractal if the union of the I_i covers $[a, b]$, each g_i maps onto $[a, b]$, and is monotonuous with derivative $|g'_i(x)| > \gamma > 1$ for all $x \in I_i$.

A fractal branching system is called linear if $g_i(x) = \beta_i x + z_i$ are linear functions. If all β_i are equal to β , we have a linear branching system with slope β . A linear branching system with $m = 2$ linear functions with slope β will be called Bernoulli system or Bernoulli convolution.

For a fractal branching system, the inverse functions $f_i = g_i^{-1} : [a, b] \rightarrow I_i$ are contractive. The family $\{f_1, \dots, f_m\}$ then forms an iterated function system with attractor $[a, b]$, cf. [9, 17]. For any choice of probabilities $p_1, \dots, p_m \geq 0$ with $\sum p_i = 1$ there is a unique probability measure ν which fulfils the equation

$$\nu(A) = \sum_{i=1}^m p_i \nu(f_i^{-1}(A)) = \sum_{i=1}^m p_i \nu(g_i(A)) \quad \text{for Borel sets } A \subset [a, b]. \quad (2)$$

For a linear branching system, Lebesgue measure can be taken as invariant measure μ , with growth factor $\sum 1/\beta_i$. If all maps have slope β , this is $\lambda = \frac{m}{\beta}$.

For a Bernoulli system, β must be between 1 and 2, and the endpoints of the interval are the fixed points of the two maps which are denoted g_0 and g_1 in this case. See Figure 1. For

each β there is only one conjugacy class of these branching dynamical systems. So z_0, z_1 can be chosen. Since we like to have the same basic interval for different values of β , we take

$$g_0(x) = \beta x, \quad g_1(x) = \beta x + 1 - \beta \quad \text{and} \quad f_0(x) = tx, \quad f_1(x) = tx + 1 - t \quad \text{on } [0, 1], \quad (3)$$

with $t = 1/\beta$. In the 1930s, the term *Bernoulli convolution* was used for the self-similar measure ν corresponding to $\{f_0, f_1\}$ and $p_1 = p_2 = \frac{1}{2}$. It is defined as the special case (1) of equation (2) mentioned in the introduction. The name comes from the fact that ν (in the version $g_0(x) = \beta x, \quad g_1(x) = \beta x - 1$ on $[0, \frac{1}{\beta-1}]$), can be expressed as an infinite convolution $\nu = \bigotimes_{n=1}^{\infty} \nu_n$ of two-point measures $\nu_n = \frac{1}{2}\delta_0 + \frac{1}{2}\delta_{t^n}$ where $t = 1/\beta$. In probabilistic terms, ν is the distribution of a random sum $\sum_n \omega_n t^n$ where all coefficients ω_n are independently chosen as 0 or 1 with probability $\frac{1}{2}$.

There are two reasons to focus on this special case. On the one hand, even Bernoulli convolutions are not well understood. On the other hand, we hope that results for the simple system will provide insight into more general cases.

For each β , or $t = 1/\beta$, the map g_0 is defined on $I_0 = [0, t]$, and g_1 on $I_1 = [1 - t, 1]$, as shown in Figure 1. The inverse maps f_0, f_1 map $[0, 1]$ onto I_0, I_1 , respectively. The intersection $D = I_0 \cap I_1$ is called overlap for the fractal construction which iterates f_0 and f_1 . We write $D_0 = f_0(D), D_1 = f_1(D)$ in Figure 7. This addressing of subintervals and points by 0-1-words and 0-1-sequences is quite common [9, 10].

3 Basic properties of finite orbits

The measure ν will now be studied for different β with the help of finite orbits. First we show that each finite orbit determines the measure $\nu(B)$ of certain intervals B .

Proposition 2 (Markov partition generated by a finite orbit)

Let $\{g_i : I_i \rightarrow [a, b] \mid i = 1, \dots, m\}$ be a fractal branching system, and let X be a finite set which contains its successors: $g_i(X) \subseteq X$ for all i . Let (p_1, \dots, p_m) be a vector of positive probabilities and ν the corresponding self-similar measure defined by (2). Then the points of X define a partition of $[a, b]$ into subintervals J_k for which $\nu(J_k)$ is uniquely determined.

Proof. Definition 2 implies that the successors of a and b are either a or b . So we add these two points to X without changing the assumptions. The points of X will be ordered, $a = x_0 < x_1 < \dots < x_n = b$. The partition intervals are $J_k = [x_{k-1}, x_k]$ for $k = 1, \dots, n$. For each i and k , the set $g_i(J_k)$ is either empty or a union of consecutive intervals J_ℓ . (Since g_i is monotonic on I_i , so in the case $x_{k-1} \in I_i, x_k \notin I_i$ either $g_i(J_k) = [g_i(x_{k-1}), 1]$ or $g_i(J_k) = [0, g_i(x_{k-1})]$. The other cases are similar.)

We now define an $n \times n$ -matrix

$$M = (m_{k\ell}) \quad \text{with} \quad m_{k\ell} = \sum \{p_i \mid J_\ell \subseteq g_i(J_k)\}$$

where $m_{k\ell} = 0$ when no i fulfils the condition. The matrix was constructed in such a way that the condition (2) for the measures $w_k = \nu(J_k)$ of the sets $A = J_k, k = 1, \dots, n$ coincides with the matrix equation $w = Mw$, that is, $w_k = \sum_\ell m_{k\ell} w_\ell$ for $k = 1, \dots, n$.

Each column sum of M equals $\sum p_i = 1$ because J_ℓ is once in $g_i(I_i)$ for each i . In other words, the vector $(1, \dots, 1)$ is a left eigenvector of M for the Perron-Frobenius eigenvalue 1. So there is a non-negative right eigenvector $w = (w_1, \dots, w_n)'$ of M , that is, a solution of $Mw = w$. To verify the uniqueness of w , we have to show that the matrix M is irreducible.

Given $k, \ell \in \{1, \dots, n\}$, we have to find a finite sequence $k_1, \dots, k_q \in \{1, \dots, n\}$ with $m_{k_{j-1}k_j} > 0$ for $j = 1, \dots, q$, with $k_0 = k, k_q = \ell$. In terms of partition intervals, this is

$$J_{k_1} \subseteq g_{i_1}(J_k), J_{k_2} \subseteq g_{i_2}(J_{k_1}), \dots, J_\ell = J_{k_q} \subseteq g_{i_q}(J_{k_{q-1}}).$$

Now since the inverse maps f_i of the g_i are contractive, there is a word $i_1 i_2 \dots i_q$ with $f_{i_1} f_{i_2} \dots f_{i_q}(J_\ell) \subseteq J_k$ (cf. [9, 17]). In other words, $J_\ell \subseteq g_{i_q} \dots g_{i_2} g_{i_1}(J_k)$. Since the g_i are strictly monotonic, $J = g_{i_{q-1}} \dots g_{i_1}(J_k)$ is an interval with endpoints in X , and we can find a subinterval $J_{k_{q-1}}$ with $J_\ell \subseteq g_{i_q}(J_{k_{q-1}}) \subseteq g_{i_q}(J)$. Recursively, the other J_{k_j} are defined. \square

If the p_i are rational, then the coefficients of the equation $Mw = w$ and the measure values $w_k = \nu(J_k)$ will also be rational. Moreover, in the case of Bernoulli convolutions the constructed irreducible Markov chain is non-periodic since $g_0(0) = 0$ implies $m_{11} = p_1 = \frac{1}{2}$.

Next, we study the growth of successor generations for a point x with finite orbit and the local dimension of ν at x . Theorem 2 below generalizes Theorem 5.2 of Baker [6]. Under special assumptions, Feng [18], Feng and Sidorov [20], and Kempton [31] have found equations or inequalities related to Theorem 2 and 3 which hold for all x , or for Lebesgue almost all x . Here we focus on finite orbits $O(x) = \{x_1, \dots, x_n\}$ in a general setting.

Let us consider the $n \times n$ successor matrix

$$S = (s_{k\ell}) \quad \text{with} \quad s_{k\ell} = |\{i \mid g_i(x_k) = x_\ell\}| \quad \text{for } k, \ell = 1, 2, \dots, n.$$

S is the adjacency matrix of a directed graph, with an edge from x_k to x_ℓ for each i with $g_i(x_k) = x_\ell$. The sum of the k -th row is the number of successors of x_k .

It is well-known and easy to check that for such an adjacency matrix, the entry $s_{k\ell}^q$ of the matrix power S^q counts the number of paths of lengths q from x_k to x_ℓ , for $q = 1, 2, 3, \dots$. Thus $s_{k\ell}^q$ is the number of compositions $g = g_{i_1} \dots g_{i_q}$ of the g_i which fulfil $g(x_k) = x_\ell$. The k -th row sum of S^q is the number $\gamma^q(x_k)$ of successors of x_k in generation q . We write $\gamma^q(x)$ instead of $|G^q(x)|$ since points are counted with multiplicity. Different g may lead to the same point.

Proposition 3 (Growth factor of a finite orbit)

If $O(x) = \{x_1, \dots, x_n\}$ is a finite orbit of a branching dynamical system with successor matrix S then the numbers $\gamma^q(x_k)$ of successors of x_1, \dots, x_n in generation q are given by the vector $S^q \cdot (1, \dots, 1)'$ for $q = 1, 2, \dots$

The growth factor $\lambda_x = \lim_{q \rightarrow \infty} \sqrt[q]{\gamma^q(x)}$ exists and equals the spectral radius $\rho(S)$. If S is irreducible, all x_j have growth factor $\rho(S)$.

Proof. The first assertion was proved above. So the row sum norm of S^q is $\|S^q\| = \max_{j=1}^n \gamma^q(x_j)$. Since each $x_j \in O(x)$ has the form $x_j = g_{i_1} \dots g_{i_r}(x)$ with $r \leq n$, we have $\gamma^{q-n}(x_j) \leq \gamma^q(x)$ for $q > n$. This implies

$$\gamma^q(x) \leq \|S^q\| \leq m^n \cdot \gamma^q(x) \quad \text{for } q > n. \quad (4)$$

Since the spectral radius of S is $\rho(S) = \lim_{q \rightarrow \infty} \sqrt[q]{\|S^q\|}$ for every matrix norm, this proves the formula for λ_x . If S is irreducible, the same argument works when x is replaced by any $y \in O(x)$. \square

For a fractal branching system and a self-similar measure ν , the growth factor can be expressed in terms of local dimension. The local dimension of a measure ν on \mathbb{R} at a point x is defined as (cf. [17])

$$d_x(\nu) = \lim_{s \rightarrow 0} \frac{\log \nu(U(x, s))}{\log s} \quad \text{where} \quad U(x, s) = [x - s, x + s].$$

Proposition 4 (Local dimension of finite orbits in branching systems of slope β)

Let $\{g_i : I_i \rightarrow [a, b] \mid i = 1, \dots, m\}$ be a linear branching system with slope β , and $O(x) = \{x_1, \dots, x_n\}$ a finite orbit which does not contain a or b . Then the local dimension at x of the self-similar measure ν with uniform probabilities $p_i = 1/m$ is

$$d_x(\nu) = \frac{\log m - \log \rho(S)}{\log \beta}$$

where $\rho(S)$ is the spectral radius of the successor matrix S of $O(x)$. If S is irreducible then all x_j have the same local dimension.

Proof. Let α be the minimum distance between $O(x)$ and $\bigcup_{i=1}^m g_i^{-1}\{a, b\}$. For each x_k, x_ℓ and each $q \geq 1$, the entry $s_{k\ell}^q$ of S^q is the number of compositions $g = g_{i_1} \dots g_{i_q}$ of the g_i which map x_k to x_ℓ . These g are linear mappings with slope β^q so they map $U(x_k, \alpha\beta^{-q})$ into $U(x_\ell, \alpha)$. According to the definition (2) of ν , iterated q times, this implies

$$\nu(U(x_k, \alpha\beta^{-q})) = m^{-q} \sum_{\ell=1}^n s_{k\ell}^q \nu(U(x_\ell, \alpha)) .$$

Now let c, C denote the minimum and maximum of the values $\nu(U(x_\ell, \alpha))$, $\ell = 1, \dots, n$, respectively. Then $\nu(U(x, \alpha\beta^{-q}))$ is between $m^{-q}\gamma^q(x)c$ and $m^{-q}\gamma^q(x)C$. Using (4) we can change the lower bound to $m^{-q}\|S^q\|cm^{-n}$ and the upper bound to $m^{-q}\|S^q\|C$. For large q we have $\frac{1}{2}\|S^q\| < \rho(S)^q < 2\|S^q\|$. Consequently,

$$\lim_{q \rightarrow \infty} \frac{1}{q} \cdot \log \nu(U(x, \alpha\beta^{-q})) = \log \rho(S) - \log m .$$

Since $\log s = \log \alpha - q \log \beta$ for $s = \alpha\beta^{-q}$, this proves the formula for $d_x(\nu)$. If S is irreducible, the argument for x holds for every x_k . \square

4 Network orbits in the Pisot case

Definition 3 (Different types of algebraic integers)

An algebraic number β is a root of a polynomial $p(x) = b_mx^m + b_{m-1}x^{m-1} + \dots + b_1x + b_0$ with integer coefficients. The degree m of p and $b_m > 0$ are chosen to be minimal, so p is unique and we can say β has degree m . If $b_m = 1$ then β is called algebraic integer. Here we consider real algebraic integers β which are greater than one. If all other roots ('conjugates') λ of p have modulus smaller than one, β is called a Pisot number. If only $|\lambda| \leq 1$ is required and equality holds for one root, then equality will hold for all conjugates, except for one real root which is $1/\beta$. In this case β is called a Salem number. If the conjugate roots only fulfil $|\lambda| < \beta$ we call β a Perron number. If only $|\lambda| \leq \beta$ is required, β is a weak Perron number. Finally, if all conjugates fulfil $|\lambda| > 1$ and $|b_0| = 2$, we call β a Garsia number.

Important Pisot parameters. The best known Pisot number is the Fibonacci or golden number $\tau = \frac{1}{2}(\sqrt{5} + 1) \approx 1.618$. More generally, for each $n \geq 2$ there is a multinacci parameter τ_n defined as positive solution of $x^n = x^{n-1} + \dots + x + 1$. The parameters $t_n = 1/\tau_n$ are the most obvious landmarks for the function Φ , shown in many of our figures. There is another family φ_n of Pisot numbers, defined as solutions $x > 1$ of $x^{n+1} = 2x^n - x + 1$

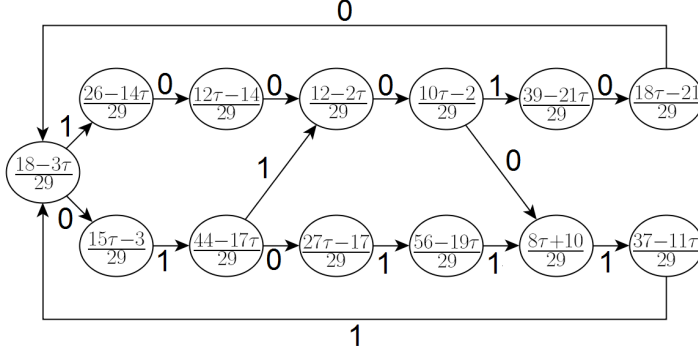


Figure 4: The orbit of $\frac{18-3\tau}{29}$ for the golden mean case

for $n \geq 2$. We call them doubling numbers and write $s_n = 1/\varphi_n$. These parameters are also indicated in our figures. Figure 1 refers to φ_2 .

The set of Pisot numbers is closed. The τ_n, φ_n for $n = 2, 3, \dots$ and a single number χ mentioned in Section 8 are the only accumulation points of Pisot numbers in $(1, 2)$. See [4] for more details and references. There are still many mysteries concerning Pisot, Salem and Garsia numbers, cf. [24]. We hope that the study of Bernoulli convolutions can shed some light on their structure.

For Garsia numbers $\beta \in (1, 2)$ it is known that the Bernoulli convolution possesses a bounded density [22]. For Pisot numbers Bernoulli convolutions are singular [15]. For all other β , including all rational numbers and Salem numbers, this question is not yet solved.

The following 'folklore theorem' says that for Pisot numbers β there are lots of network-type orbits. Garsia [22] found the basic property, a uniform discreteness lemma, which was recently used by Baker [6] to verify the statement. Schmidt [40] proved a special case with other estimates. A direct proof is given in the first arxiv version of this paper.

Theorem 5 (Abundance of finite orbits for Pisot slope [22, 40])

Let $g_i(x) = \beta x + z_i$, $i = 1, \dots, k$ be a branching dynamical system on an interval $[a, b]$. If β is a Pisot number and each z_i is in $\mathbb{Q}(\beta)$, then $O(x)$ is a finite set for each x in $\mathbb{Q}(\beta)$.

The Bernoulli convolution for the Fibonacci parameter was studied by many authors [1, 18, 20, 27, 34, 45], with focus on the dimension and multifractal spectrum of the measure. Here we consider periodic orbits for $g_0(x) = \tau x$, $g_1(x) = \tau x + 1 - \tau$ to illustrate our subject. The point $x = \frac{1}{2}$ has period 3, it fulfils $g_{100}(x) = g_{011}(x) = x$. Thus the orbit $O(x)$ consists of five points, and the growth factor is $\sqrt[3]{2} \approx 1.2599$. By Proposition 4, the local dimension of the Bernoulli measure at $\frac{1}{2}$ is 0.9603. A slightly more complicated case is shown in Figure 4. The point $x = \frac{18-3\tau}{29}$ has the fixed period 7, and it has 5 successors in generation 7. The growth rate is $\sqrt[7]{5} \approx 1.2585$, and the local dimension is 0.9626.

These two networks have a special structure. Let us say that a directed graph is a *cycle mixture* of period p if all minimal directed cycles in the graph have length p , and each edge is contained in a cycle. A vertex v_0 which is contained in all cycles of the mixture will be called *root*. Let m denote the number of cycles. If there is a root, the number of successors of v_0 in generation $p \cdot k$ is m^k for $k = 1, 2, \dots$. So the growth factor is $\rho = \sqrt[p]{m}$, cf. Proposition 3.

Two cycle mixtures with root vertices v_0, v'_0 can be concatenated by redirecting all incoming edges of v_0 to V'_0 , and all incoming edges of v'_0 to v_0 . The period of the concatenated

graph will be $p + p'$, and the number of minimal cycles $m \cdot m'$. Given two cycle mixtures, repetition of this product construction will lead to infinitely many other examples. Let us say that a cycle mixture is *prime* if it contains exactly one root vertex, and thus is not obtained by concatenation. For the Fibonacci parameter, there are prime cycle mixtures of arbitrary large complexity.

Theorem 6 (Finite orbits with large complexity in the Fibonacci case)

For each odd period $p = 2k - 1, k \geq 1$, the golden Bernoulli convolution admits a prime cycle mixture with $n = 4k - 3$ points and $m = F_{k+1}$ cycles, where $F_1 = F_2 = 1, F_3 = 2, \dots$ denote the Fibonacci numbers. For $k \rightarrow \infty$ the growth rates $\rho_k = \sqrt[p]{m}$ of these orbits converge to the maximum growth rate $\sqrt{\tau}$.

The cases $p = 3$ and $p = 7$ were discussed above. The general construction is given at the end of Section 6. Note that the F_k increase exponentially. Already for $p = 15$, we get $F_9 = 34$ cycles while the five-fold concatenation of two intersecting 3-cycles would provide only $2^5 = 32$ cycles. For $p = 29$ we obtain 987 cycles on a basic set of 57 points.

For even periods, however, we get cycle mixtures without root, as seen on the left of Figure 5 for $p = 4$. Pisot parameters β of higher degree, with conjugates nearer to the unit circle, admit much more complicated networks, cf. Section 10. Theorem 6 gives only an impression of how complicated finite orbits can be.

The convergence $\sqrt[p]{F_{k+1}} \rightarrow \sqrt{\tau}$ follows from $F_k \approx \tau^k / \sqrt{5}$. The minimum local dimension of ν_t for the Fibonacci case was found by Hu [27], cf. [18]. The corresponding growth rate $\sqrt{\tau} \approx 1.2720$ is realized by the orbit of $x = \frac{2\tau-1}{5} = 1/\sqrt{5}$ shown on the left of Figure 5. One image of x goes to $1 - x$ after two steps, the other returns to x after four generations. The growth rate ρ fulfils the equation $\rho^4 = \rho^2 + 1$ (due to symmetry, the spectral radius can be determined for a graph with 4 vertices). Thus $\rho = \sqrt{\tau}$, with local dimension 0.9404. In Section 10 we shall see that such double orbits combining x with $1 - x$ often yield large growth rates. We briefly prove that the growth rate $\sqrt{\tau}$ is indeed maximal.

For $\beta = \tau$, the two successors of a point in the overlapping set D will either both return after 3 generations, as for $x = \frac{1}{2}$, or will return after 2 and ≥ 4 generations, as in Figure 5, or will return later. The case with 2 and 4 gives the highest growth, and Figure 5 shows that this case can be iterated with itself forever, so this yields the maximum growth rate. Many other finite orbits combine the 3-3-return with the 2-4-return so that the growth rate is between $\sqrt[3]{2}$ and $\sqrt{\tau}$.

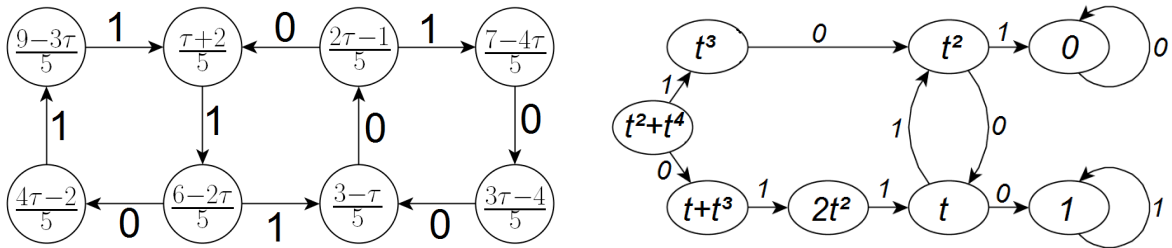


Figure 5: Orbits with maximum and minimum growth rate

On the right of Figure 5 we show the preperiodic orbit of $x = t_2^2 + t_2^4$. Both image points of x eventually land in the fixed points 0 or 1. For each point in this orbit, the number of

successors in generation q grows linearly with q , so the growth rate assumes its minimal value 1. The local dimension becomes $\frac{\log 2}{\log \tau} \approx 1.4404$. Such examples are discussed in Sections 7-9.

In a histogram approximating the Fibonacci measure, similar to Figure 1, the bars for points with local dimension < 1 should be very high, and the bins of points with local dimension > 1 should show very small values. However, since the minimum local dimension is 0.9404, the high values, 'poles of the singular measure', can hardly be recognized. With a maximum local dimension of 1.4404, the zeros of the measure are much more apparent. In our figures this effect is obvious for β near τ . When β tends to 2, however, the maximum local dimension approaches 1, minimal values are difficult to recognize and large values are better visible.

5 Network orbits require weak Perron slope

In general, network orbits in a branching dynamical system are exceptions. The condition that x will repeat in its orbit is an equation of the form $g_{w_n} \cdot \dots \cdot g_{w_1}(x) = x$. Two equations of this type for the same point x will severely restrict the choice of mappings. This will be made precise for the case of Bernoulli convolutions. The first part of our statement is related to Sidorov's Theorem 2.1 and Proposition 2.6 in [44] and Theorem 3.6 in [43]. The role of Perron numbers was emphasized by Thurston [48]. He proved that weak Perron numbers β are in one-to-one correspondence $\beta = \exp(h)$ with topological entropies h of maps from $[0, 1]$ to itself with finitely many turning points which have finite orbits. The second part of our theorem was indicated by the remarks after Theorem 1.2 in [48].

Theorem 7 (Condition for existence of network orbits)

Suppose that in a Bernoulli convolution with slope β there is a point y such that the orbit of y contains two different paths from y to cycles or finite invariant sets. Then β must be an algebraic integer. If the orbit of y is finite then β is a weak Perron number.

Proof. Without loss of generality we assume that the two paths differ at the first step. Thus y belongs to the overlap region, and both $g_0(y)$ and $g_1(y)$ lead to a cycle or periodic component. If y itself is not periodic, there are 0-1-words v, w, v', w' with $v_1 \neq v'_1$ and

$$g_w(x) = x \quad \text{for} \quad x = g_v(y) \quad \text{and} \quad g_{w'}(x') = x' \quad \text{for} \quad x' = g_{v'}(y) .$$

Without loss of generality we assume that the length m of the word v is not smaller than the length m' of v' . When y itself is periodic we have the special case that either v' is the empty word, $y = x'$ and $w'_1 \neq v_1$, or both v and v' are empty, $y = x = x'$ and $w'_1 \neq w_1$. We shall call this the single period and double period case, respectively.

For $w = w_1 \dots w_n \in \{0, 1\}^n$ we have $g_w(x) = g_{w_n} \cdot \dots \cdot g_{w_1}(x) = \beta^n x + (1 - \beta) \sum_{i=1}^n \beta^{n-i} w_i$. We solve $g_w(x) = x$ for x and $g_{w'}(x') = x'$ with $w' = w'_1 \dots w'_{n'}$ for x' .

$$x = \frac{\beta - 1}{\beta^n - 1} \sum_{i=1}^n \beta^{n-i} w_i \quad \text{and} \quad x' = \frac{\beta - 1}{\beta^{n'} - 1} \sum_{i=1}^{n'} \beta^{n'-i} w'_i .$$

The equation $x = g_v(y) = \beta^m y - (\beta - 1) \sum_{j=1}^m \beta^{m-j} v_j$ with $v = v_1 \dots v_m$ and $x' = g_{v'}(y)$ with $v' = v'_1 \dots v'_{m'}$ are both solved for y :

$$\frac{1}{\beta^m} (x + (\beta - 1) \sum_{j=1}^m \beta^{m-j} v_j) = y = \frac{1}{\beta^{m'}} (x' + (\beta - 1) \sum_{j=1}^{m'} \beta^{m'-j} v'_j) .$$

We multiply both sides with β^m , substitute x and x' and cancel $\beta - 1$:

$$\frac{1}{\beta^n - 1} \cdot \sum_{i=1}^n \beta^{n-i} w_i + \sum_{j=1}^m \beta^{m-j} v_j = \beta^{m-m'} \left(\frac{1}{\beta^{n'} - 1} \cdot \sum_{i=1}^{n'} \beta^{n'-i} w'_i + \sum_{j=1}^{m'} \beta^{m-j} v'_j \right) .$$

Multiplying with $\beta^n - 1$ and $\beta^{n'} - 1$ we obtain polynomials with integer coefficients.

$$\begin{aligned} (\beta^{n'} - 1) \left(\sum_{i=1}^n \beta^{n-i} w_i + (\beta^n - 1) \sum_{j=1}^m \beta^{m-j} v_j \right) = \\ (\beta^n - 1) \beta^{m-m'} \left(\sum_{i=1}^{n'} \beta^{n'-i} w'_i + (\beta^{n'} - 1) \sum_{j=1}^{m'} \beta^{m-j} v'_j \right) . \end{aligned} \quad (5)$$

With $N = n + n' - 1$, the leading terms are

$$\beta^N w_1 - \beta^{N+m} v_1 \quad \text{on the left side and} \quad \beta^{N+m-m'} w'_1 - \beta^{N+m} v'_1 \quad \text{on the right side.}$$

If $m' \geq 1$, then $m \geq 1$ because of $m \geq m'$, and the leading exponent $N + m$ is greater N and $N + m - m'$. The coefficients v_1 and v'_1 of β^{N+m} on both sides differ by 1 according to the assumption of the theorem, so β is the root of a polynomial with integer coefficients and leading coefficient 1.

If $m' = 0$, we have $y = x'$ and the sum with v'_j on the right disappears. For the single period case $m > 0$, the leading term $N + m$ has coefficients v_1 and w'_1 which now must be different, zero and one. For the double period case $m = 0$, the v_i also disappear and we are left with coefficients w_1 and w'_1 for the leading term β^N , which in this case must differ since they correspond to application of g_0 and g_1 to y in the first step. In all cases the leading coefficient is ± 1 , so β is an algebraic integer. The first part of the proof is complete.

Remark. Not all choices of words v, w, v', w' are possible in Bernoulli convolutions since equation (5) will not always have a solution in $(1, 2)$. This will be clarified below. Moreover, without further assumptions on y we cannot expect that β will become a weak Perron number. Already the double period case with $n = n'$ and arbitrary w, w' leads to all polynomials with coefficients in $\{-1, 0, 1\}$, and $p(x) = x^7 - x^5 + x^3 - x^2 - 1$ has a real root at 1.166 and complex roots with modulus 1.24.

For the proof that β is weak Perron, we need not require that the whole orbit of y is finite. Let h be the function on $[0, 1]$ with $h(x) = g_0(x)$ for $x < y$ and $h(x) = g_1(x)$ for $x > y$. Only $h(y) = \{g_0(y), g_1(y)\}$ is two-valued. We assume that the orbit of y under h is finite. Since $g_0(z) > z$ and $g_1(z) < z$ for all z , the orbit can be written in ordered form as $g_1(y) = x_0 < x_1 < \dots < x_n = g_0(y)$, and $y = x_k$ with $0 < k < n$. We let $J_i = [x_{i-1}, x_i]$ for $i = 1, \dots, n$ and define a matrix

$$M = (m_{ij}) \quad \text{with} \quad m_{ij} = 1 \quad \text{if } J_j \subseteq h(J_i) \quad \text{and} \quad m_{ij} = 0 \quad \text{otherwise.}$$

M is the adjacency matrix of a graph where an edge leads from i to j whenever $J_j \subseteq h(J_i)$. Since at least one edge starts from each i , there is a vertex set $W \subseteq \{1, \dots, n\}$ such that no edge leads from W to other vertices, and for any two vertices $i, j \in W$ there is a directed path from i to j . (Write $i \preceq j$ if $i = j$ or there is a directed path from i to j , and let $i \sim j$ if

$i \preceq j$ and $j \preceq i$. Take a maximal element i^* with respect to \preceq and let W be the equivalence class of i^* .)

So the adjacency matrix $M_W = (m_{ij})_{i,j \in W}$ of the subgraph induced by W is irreducible. Since the length of $h(J_i)$ is β times the length of J_i , the vector of lengths of the J_i with $i \in W$ is an eigenvector of M_W with eigenvalue β . By the theorem of Perron and Frobenius this implies that β is a weak Perron number. \square

Remark. One can show $W = \{1, \dots, n\}$ but this is not needed here. We do not know whether β must be a Perron number when y has finite orbit under $\{g_0, g_1\}$. Under the weaker assumption that y has finite orbit under h , this will not hold, as shown by the example of $y = \frac{1}{2}$ for $\beta = \sqrt{2}$.

6 The parametric family of Bernoulli convolutions

We now resume the discussion of the parametric family of Bernoulli measures in the introduction. As known from other families of dynamical systems, e.g. the logistic family and the Mandelbrot set [11, 36, 37], there is a lot of repetition and number theory which generates some structure in an otherwise chaotic picture. In our case, the number theory involves algebraic integers, mainly Pisot numbers. It will turn out that basic features of the complete family of Bernoulli convolutions are easier to understand than single specimen like Figure 1.

We recall the fractal construction of the Bernoulli measure ν_t , using the contracting similitudes $f_0(x) = tx$ and $f_1(x) = tx + 1 - t$ on $I = [0, 1]$ which are the inverse maps of g_0, g_1 . In the first step we consider the intervals $I_0 = f_0(I) = [0, t]$ and $I_1 = f_1(I) = [1 - t, 1]$ and the probability density $\phi^1(x) = \frac{1}{2t}(1_{I_0}(x) + 1_{I_1}(x))$ which is piecewise constant. When we assume $t > \frac{1}{2}$, there is a overlap interval $D = I_0 \cap I_1 = [1 - t, t]$ on which ϕ^1 assumes the value $\frac{1}{t}$. In the second step, we consider intervals $I_{00}, I_{01} = f_0 f_1(I)$ etc., and we will have new overlap intervals $D_0 = f_0(D) = I_{00} \cap I_{01}$ and D_1 . In step k , we consider words $w = w_1 \dots w_k \in \{0, 1\}^k$, contractions $f_w = f_{w_1} \dots f_{w_k}$, and corresponding intervals $I_w = f_w(I)$. The approximating density of ν_t on level k can be written as $\phi^k(x) = (2t)^{-k} \sum_w 1_{I_w}(x)$ where the sum runs over all 01-words of length k . That is, we count how many intervals I_w contain the point x . It is easy to see that this is just the number of successors of x in generation k with respect to the branching dynamical system $G = \{g_0, g_1\}$. The normalizing factor $(2t)^{-k}$ is needed to obtain a probability measure. Hutchinson has shown that the measures given by the densities ϕ^k converge to ν_t in the space of probability measures with a metric which nowadays is usually called transport distance. See [26, 17, 9] for more details.

There is another interpretation which uses the space $\Sigma = \{0, 1\}^\infty$ of 01-sequences $s = s_1 s_2 \dots$. For each sequence s there is a point $x = \pi(s) \in [0, 1]$ which can be written as $x = \lim_{k \rightarrow \infty} f_{s_1} \dots f_{s_k}(0)$. The mapping $\pi : \Sigma \rightarrow [0, 1]$ is continuous. Again, we refer to [26, 17, 9]. We say that x has address $s = s_1 s_2 \dots$. In an overlapping system, a point can have many addresses. Let μ denote the product measure on Σ given by $p_0 = p_1 = \frac{1}{2}$. In probability theory, μ models a sequence of independent coin tosses. Here, it is considered the equidistribution of addresses. The measure ν_t measures how many addresses the points $x \in [0, 1]$ have: $\nu_t = \mu \cdot \pi^{-1}$ is the image measure of μ under the address map π .

On the level k , it is natural to count for each x the number of words $w = w_1 \dots w_k$ which can be extended to an address of x . This number, multiplied by the normalizing factor $(2t)^{-k}$, is equal to $\phi^k(x)$. Thus $\phi^k(x)$ has three interpretations:

- the number of intervals I_w on level k which contain x ,

- the number of successors of x in generation k with respect to the system $G = \{g_0, g_1\}$,
- the number of prefixes of length k of addresses of x .

The density functions $\phi^k(x)$ represent approximations of ν_t which converge to ν_t for $k \rightarrow \infty$. Convergence in the transport distance d is fast, $d(\phi^k, \nu_t) \leq t^k \cdot d(\phi^0, \nu_t)$ where ϕ^0 is the equidistribution on $[0, 1]$. However, ν_t need not be given by a density function.

These facts hold for all t between 0 and 1, and we shall study ν_t for all $t \in [\frac{1}{2}, 1)$ of the overlapping case together. In Figure 2 the Bernoulli measures ν_t for $0.5 \leq t \leq 0.76$ are represented by approximate densities ϕ^k with $k = 26$, which themselves were approximated by histograms with 4000 bins. For most figures, a Markov chain model was used. Numerical methods will be discussed elsewhere. Our aim here is to understand the measures analytically.

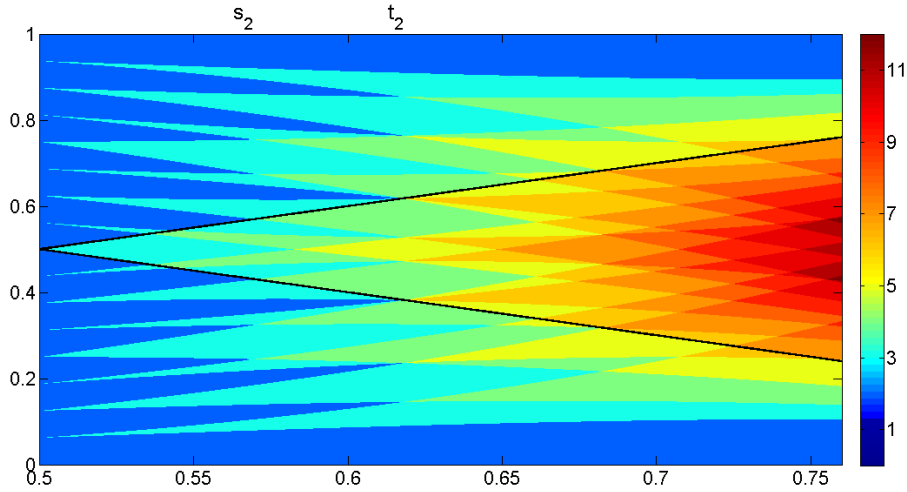


Figure 6: Low-level approximation $\phi_t(x)$ of Figure 2. For each parameter t in $[0.5, 0.76]$, each point x is assigned the number of pieces I_w on level $k = 4$ which contain x , shown by color code. The black lines $x = t$ and $x = 1 - t$ mark the border of the main overlap region \mathbf{D} .

To this end, we show in Figure 6 the function $\phi_t^k(x)$ on the smaller level $k = 4$. The normalizing factor is omitted to clarify the combinatorial structure. Possible values are the integers $1, \dots, 16$. For t near to 1, all 16 intervals will contain the point $x = \frac{1}{2}$, but for $t \leq 0.76$ at most 11 intervals intersect each other. The number of intersections decreases when t becomes smaller. For $t < \frac{1}{2}$ all intervals I_w within the same level are disjoint. For x near to the endpoints the value of ϕ is 1 since 0 is contained only in $I_{0\dots 0}$ and 1 only in $I_{1\dots 1}$. On the other hand, we have the big triangular overlap region $\mathbf{D} = \{(t, x) \mid t \leq x \leq 1 - t\}$ where two intervals meet already on the first level. We have other 'horns' $\mathbf{D}_0 = f_0(\mathbf{D})$, $\mathbf{D}_w = f_w(\mathbf{D})$ where intervals meet on levels 2, 3, 4. More rigorously, we define $\mathbf{D}_w = \{(t, x) \mid f_w(t) \leq x \leq f_w(1 - t)\}$ and note that this is a curvilinear triangle with tip at $(\frac{1}{2}, f_w(\frac{1}{2}))$ and base line $\{(1, x) \mid 0 \leq x \leq 1\}$ outside Figure 6. Where horns intersect, the value of ϕ increases accordingly. This mainly happens for large t and for points x near $\frac{1}{2}$. One could think that the maximum of $\phi_t(x)$ is always at $x = \frac{1}{2}$ but for many t this is not the case. The combinatorics of intersections of horns seems complicated.

While the intersections of horns indicate regions with many addresses, there are dark regions with baseline on the left border $t = \frac{1}{2}$ in Figure 6 which represent the points with only one address. It is interesting that their tips are at the golden mean parameter $t_2 = \frac{1}{\tau} \approx 0.618$

with $\tau = \frac{1}{2}(\sqrt{5} + 1) \approx 1.618$ or smaller t , like $t = s_2 \approx 0.57$. When the level k grows, these regions must become smaller, but they will not disappear completely.

Let us turn to level 26, Figure 2. Horns $f_w(\mathbf{D})$ are still visible, but the dark regions on the left have become very thin. The golden mean $t_2 \approx 0.618$ apparently marks a phase transition. For $t < t_2$, there is a lot of structure. For $t > t_2$, this structure becomes blurred, and only few details are apparent. The interval for t was chosen to include all inverses of Pisot numbers $\beta \in [1, 2]$. The first and second Pisot numbers, 1.3247 and 1.3803, can be recognized in Figure 2 at $t \approx 0.755$ and 0.725, respectively. The next two Pisot numbers are vaguely visible at 0.693 and 0.682.

In this note, we shall focus on the region $\frac{1}{2} \leq t \leq t_2$ where the structure seems most apparent. Because of the symmetry of the measures ν_t we restrict our study to points $x \leq \frac{1}{2}$. Repetitions in Figure 2 at the lower and upper border are caused by the definition of ν_t . In (1) one term on the right disappears when A does not intersect the overlap interval D since either g_0 or g_1 do not apply to A . We have

$$\nu_t(g_0(A)) = 2\nu_t(A) \text{ for } A \subseteq [0, 1-t] \quad \text{and} \quad \nu_t(g_1(A)) = 2\nu_t(A) \text{ for } A \subseteq [t, 1]. \quad (6)$$

For this reason, Figure 7 was restricted to $\frac{1}{2} \leq t \leq 0.63$, $0.325 \leq x \leq 0.5$. Again, each ν_t was approximated by a histogram of the density ϕ_t^{26} with 4000 bins, standardized so that the integral over $[0, 1]$ is 1. As shown in the scale bar on the right, numerical values of densities on this approximation level vary only between zero and four, even though some ν_t are known to be singular.

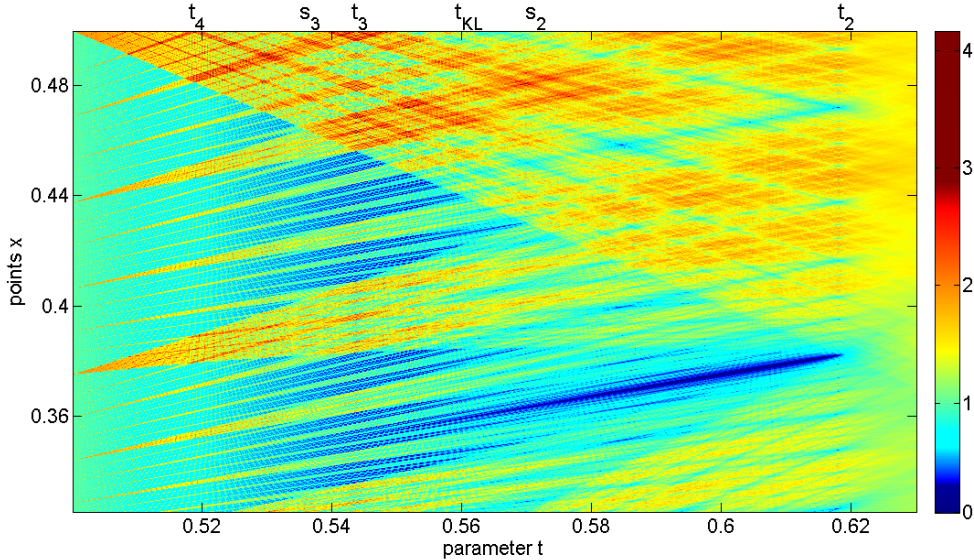


Figure 7: Φ for $0.5 \leq t \leq 0.63$, $0.325 \leq x \leq 0.5$. Right of the golden mean, the structure becomes blurred. On the left, periodic points appear outside \mathbf{D} , starting at $t_2 \approx 0.618$ with the dark curve which hits the y -axis at $1/3$.

In Figure 7 we see again that for $t > t_2$ the structure becomes blurred. The same is true for t near $\frac{1}{2}$ where the ν_t converge to the uniform distribution. The most obvious feature are the dark curves which lead from the left border upwards and end just outside the overlap region \mathbf{D} , which here is the upper triangle with large density values. These curves indicate points with unique address which have been studied by many authors and will be dealt with

in the next section. In Section 8 and 9, we shall consider the blue and red crossing points inside the overlap region which are related to singularity of the measures ν_t . Periodic points will play a key role in our investigation.

Note that for all words $w = w_1 \dots w_n$, the map f_w is the inverse of g_w . To avoid reverse words, we use the convention that $g_w = g_{w_n} \dots g_{w_1}$ while $f_w = f_{w_1} \dots f_{w_n}$. Thus

$$f_w(x) = t^n x + (1 - t) \cdot \sum_{k=0}^{n-1} w_k t^k \quad (7)$$

which for $n \rightarrow \infty$ leads to the address curves of points defined below. For fixed word length, the map f_w describes the piece $I_w = f_w(I)$ of level n . Since pieces overlap, they can also coincide, which is called 'exact overlap', and has been considered a main reason for singularity of ν_t [22]. Clearly, $I_w = I_v$ if and only if $f_w = f_v$, and this can happen only if w and v have the same length n . In this case the maps coincide iff $f_w(0) = f_v(0)$ iff the fixed points coincide, that is $f_w(0)/(1 - t^n) = f_v(0)/(1 - t^n)$ by equation (7).

The Fibonacci case - Proof of Theorem 6. For $t = t_2$ the characteristic equation is $1 = t + t^2$. In terms of mappings this means $f_{100} = f_{011}$. Thus the orbit of the fixed point $x = \frac{1}{2}$ of this mapping under $G = \{g_0, g_1\}$ consist of two 3-cycles: $x, g_0(x) = f_{11}(x), g_{01}(x) = f_1(x)$ and $x, g_1(x), g_{10}(x)$. Moreover, for all words u, v we have $f_{u100} = f_{u011}$ as well as $f_{100v} = f_{011v}$, by (7).

Taking $u = 10, v = 00$ we conclude that the pieces I_w and maps f_w coincide for the words 10000, 01100, 01011. The orbit of the fixed point of this map is a cycle mixture with $p = 5, m = 3$. Since 2 of the words end with 0, and only one with 1, we next take $v = 11$ and obtain $m = 5$ words of length $p = 7$ describing the same piece and map: 1000011, 1000100, 0110011, 0110100, 0101111. The corresponding orbit is shown in Figure 4.

Thus what we called 'cycle mixture with root' is just a description of exact overlap of m pieces on level p . The $2p - 1$ vertices of the graph represent the pieces of lower level which contain this overlap piece: on each level there are *exactly two choices*, except for the initial stage where we only have the interval I . For the last two levels, the overlap piece is just the intersection of the two larger pieces:

$$I_{100} = I_{10} \cap I_{01} = I_1 \cap I_0 \quad . \quad I_{10000} = I_{1000} \cap I_{0101} = I_{100} \cap I_{010} \quad . \quad (8)$$

We extend the construction by induction. Suppose we have $m = F_{k+1}$ words w of length $p = 2k - 1$ describing the same map, and suppose that F_k of the words end with 0 and F_{k-1} end with 1, to be definite (every second step we interchange 0 and 1). Now take all words $w11$, and add the words of the first type where the terminal 0 was replaced by 100. These are $F_{k+1} + F_k = F_{k+2}$ words which all describe the same piece J of level $p + 2$, and F_{k+1} of them end with 1. Let w' obtained from one word w of first kind by replacing the terminal 0 by 1. Then on levels p and $p + 1$ there are only two pieces which contain J , namely $J = I_w \cap I_{w'} = I_{w1} \cap I_{w'0}$, by (8) and self-similarity. In each induction step, the period (or level) grows by 2, the number points (or larger pieces) by 4, and the number of cycles (or words for the overlap turns to the next Fibonacci number, that is roughly multiplication by τ . \square

Instead of alternatingly extending words by 00 and 11, we can make a random choice in each induction step. This will generate other finite orbits with the same period and same number of points, but with a smaller number of cycles, for instance $m = 4$ for $p = 7$, and thus with a smaller growth rate.

7 Points with unique addresses

Now we consider points x which have a unique address $\pi^{-1}(x)$ in the fractal construction of ν_t . In other words, for each level k , the point x belongs to a single piece I_w of level k . In terms of our branching dynamical system $G = \{g_0, g_1\}$, there is only one successor of x for each level k . That is, repeated images of x by g_0 and g_1 will never hit the overlap interval $D = [t, 1 - t]$. Typical examples are the points $x = 0$ with address $000\dots = \bar{0}$ and $x = 1$ with address $\bar{1}$, for any $t < 1$.

The curves for period 2. Erdős, Joó, and Komornik noted around 1990 that there are no other points with unique address when t is larger or equal the golden mean parameter t_2 . The overlap interval \mathbf{D} and its images $\mathbf{D}_{0^k}, \mathbf{D}_{1^k}$ with $k = 1, 2, \dots$ will cover the whole interval $(0, 1)$. As a consequence, each point $x \in (0, 1)$ has a continuum of addresses [16, 43]. For $t < t_2$, however, the points

$$y = \frac{t}{1+t} < t \text{ and } z = 1 - y = \frac{1}{1+t} > 1 - t \quad \text{fulfil} \quad g_0(y) = z \text{ and } g_1(z) = y. \quad (9)$$

So their orbits avoid D , and they have unique addresses $\overline{01}$ and $\overline{10}$. They form a periodic orbit of length 2 for $t < t_2$. For $t = t_2$, the points y and z are on the boundary of D and have a countable number of addresses, as is easy to check.

If a point x has a finite or countable number of addresses, the growth rate of its successors is $\rho = 0$ and by Proposition 4, the local dimension of ν at x equals $\frac{\log 2}{\log \beta} > 1$. The density of ν at x is $\lim_{\epsilon \rightarrow 0} \frac{\nu[x-\epsilon, x+\epsilon]}{2\epsilon} = 0$. For this reason, points with unique addresses indicate themselves by dark blue color in our figures. The curve $y = y(t)$ for $\frac{1}{2} \leq t \leq t_2$ is apparent in Figure 7, in particular for t near t_2 where the local dimension is 1.44 while for $t \rightarrow \frac{1}{2}$ it tends to 1. Our big Figure 2 shows the dark curves $y(t), z(t) = 1 - y(t)$, and their images under the contractions f_0 and f_1 , that is, $t^k y(t)$ and $1 - t^k y(t)$ for $k = 1, 2, \dots$

Curves for period 4. There are many other points with unique address when t becomes smaller! The overlap region will then be smaller and other periodic points appear outside D . As Figure 6 indicates, the next parameter where a point with unique address separates from \mathbf{D} is around 0.57. At $t = s_2 \approx .5698$, the inverse of the Pisot number $\sigma \approx 1.7549$ with minimal polynomial $\beta^3 - 2\beta^2 + \beta - 1$ (Figure 1), the equation $g_{1001}(t) = t$ holds. For $t < s_2$ we have the following periodic orbit of length 4 outside the overlap region D .

$$\frac{t^2}{1+t^2}, \frac{t}{1+t^2}, 1 - \frac{t}{1+t^2}, \frac{1}{1+t^2} \quad (10)$$

The unique addresses of these points are $\overline{0011}, \overline{0110}, \overline{1001}, \overline{1100}$. For $t \in [\frac{1}{2}, s_2)$, formula (10) defines four curves of points with unique address, density zero and maximal local dimension $\frac{\log 2}{\log \beta}$ which indicate themselves in our figures by their dark blue color. There are many image curves under contraction maps f_w – any of the address curves $t^k y(t)$ of period 2 will on $[\frac{1}{2}, s_2)$ be an ‘accumulation point’ of such curves. For $k = 2$, the curves with addresses $00(01)^n \overline{0110}$ and $00(01)^n \overline{0011}$ will for $n \rightarrow \infty$ converge from both sides to the curve with address $000\bar{1}$.

The basic doubling scenario. For $s_2 < t < t_2$, however, no further points with unique address exist because for these parameters, the horn $\mathbf{D}_{(01)^k}$ with $k = 1, 2, \dots$ will cover the area between the curve $y(t)$ and the main horn \mathbf{D} in Figures 6,7. The parameters $t \leq t_2$ where new points with unique addresses appear form a decreasing sequence connected with the addresses $\overline{01}, \overline{0110}, \overline{01101001}, \overline{0110100110010110}$. The addresses converge to the well-known Morse-Thue sequence, and the t -values converge to a parameter $t_{KL} \approx .5595$ found by Komornik and Loreti [33] and shown to be transcendental by Allouche and Cosnard [3].

The sets A_t . For each $t > t_{KL}$ the set A_t of points with unique addresses is countable, for $t \leq t_{KL}$ it is uncountable. Starting with basic contributions of Daroczy and Katai [13], Glendinning and Sidorov [23] and Kallós [30] many authors have studied the topological structure of A_t and the Hausdorff dimension of A_t . The work of de Vries and Komornik [14] collects results up to 2009. More recent papers include Sidorov [44], Jordan, Shmerkin and Solomyak [29], Kong and Li [32], and Baker [6]. The study of sets A_t was inspired by work on univoque numbers [12, 4, 33, 14] which will be discussed below.

Connection with one-dimensional dynamics. The doubling scenario with the Morse-Thue sequence is known from the dynamics of one-dimensional unimodal maps, where Milnor and Thurston used a bit different type of address [36, 11], and from the binary coding of exterior angles of the Mandelbrot set, cf. [37], where exactly the addressing is the same as here. The words 01, 0110, ... describe bubbles of the Mandelbrot set which hit the real axis. Here they describe horns which intersect the main horn \mathbf{D} . A related result of Allouche, Clarke and Sidorov [2] says that the Sharkovskii ordering of periodic points in one-dimensional maps agrees with the ordering of periodic points outside the overlap region which arise for decreasing t . Another analogy with continued fractions was recently found by Tiozzo and co-authors, see [49].

It is easy to explain the reason for the connection between Bernoulli convolutions and one-dimensional real and complex maps. The doubling map $g : [0, 1) \rightarrow [0, 1)$ is defined by

$$g(x) = 2x \bmod 1, \quad \text{that is, } g(x) = 2x \text{ for } 0 \leq x < \frac{1}{2} \quad \text{and} \quad g(x) = 2x - 1 \text{ for } \frac{1}{2} \leq x < 1.$$

In complex dynamics it is proved that the map $h(z) = z^2 + c$ induces the map g on the external rays of the Julia set for each c , and thus on the external rays of the Mandelbrot set. This was a basic fact for the studies of quadratic maps by Douady, Hubbard and Thurston in the 1980s, cf. [37].

In our context, the following basic statement says that g is conjugate to the dynamics of $G = \{g_0, g_1\}$ for each $t < t_2$ and for all points x which have their image outside D . In other words, g describes the dynamics of G where it is single-valued, for each possible t .

Proposition 8 (Conjugacy of Bernoulli and doubling map)

Let $t \in (\frac{1}{2}, 1)$, and let F_t denote the cumulative distribution function of ν_t , which means $F_t(x) = \nu_t[0, x]$ for $0 \leq x \leq 1$. Then F_t defines a conjugacy between the action of G on $[0, 1] \setminus D$ and the doubling map g on a corresponding subset of $[0, 1]$. That is,

$$F_t \cdot G(x) = g \cdot F_t(x) \quad \text{for } x \in [0, 1] \setminus D.$$

Proof. We use the special case (6) of the definition of ν_t . For $x < 1 - t$ we get

$$F_t g_0(x) = \nu_t[0, g_0(x)] = \nu_t(g_0[0, x]) = 2\nu_t[0, x] = gF_t(x).$$

For $x > t$ we have $G(x) = g_1(x)$ and $F_t g_1(x)$ is transformed as follows;

$$\nu_t[0, g_1(x)] = 1 - \nu_t[g_1(x), 1] = 1 - \nu_t(g_1[x, 1]) = 1 - 2\nu_t[x, 1] = 2F_t(x) - 1 = gF_t(x). \quad \square$$

In order to get a conjugacy between dynamical systems, we have to restrict ourselves to points x for which the orbit under G does not intersect D . This means that x has unique address and implies $t \leq t_2 \approx 0.618$. Let us recall the Milnor-Thurston concepts of itinerary

and kneading sequence, for our case of the doubling map. Following seminal work by Parry 1960, these 01-sequences were widely used in connection with β -expansions, see for example [16, 23, 4, 14]. Binary numbers have the advantage that eventually periodic sequences are identified with rational numbers, and the simple arithmetic of the doubling map g can be used, as it is done for the external angles of the Mandelbrot set [37]. g acts as shift map on binary representations of numbers in $[0, 1]$.

Definition 4 (Binary itineraries, kneading sequences, address curves)

A 01-sequence $b_1b_2\dots$ and the corresponding binary number $b = .b_1b_2\dots = \sum_{k=1}^{\infty} b_k 2^{-k}$ are called *itinerary* if the orbit closure of b under the doubling map does not contain the point $\frac{1}{2}$. If b itself realizes the minimal distance, that is, no number $g^{(k)}(b) = .b_kb_{k+1}\dots$ with $k = 1, 2, \dots$ is nearer to $\frac{1}{2}$ than b , we call b a *kneading sequence*. For each itinerary b , the function

$$y_b(t) = \frac{1-t}{t} \cdot \sum_{k=1}^{\infty} b_k t^k \quad (11)$$

is called the *address curve* corresponding to b .

Binary itineraries are exactly those 01-sequences which do not have neither $\bar{0}$ nor $\bar{1}$ in their orbit closure under the shift (recall that $\frac{1}{2}$ has the binary addresses $1\bar{0}$ and $0\bar{1}$). In other words, these sequences do not contain n consecutive equal symbols 0 or 1, for some integer n . The kneading sequence corresponding to a given itinerary b can be obtained by determining the orbit closure of $.b_1b_2\dots$ under the doubling map, and taking the point (or one of the two points) nearest to $\frac{1}{2}$. If b itself is a kneading sequence, then so is $1-b$. So it suffices to study the case $b < \frac{1}{2}$, that is, $b_1 = 0$.

The parameter t^* . For a kneading sequence b with $b_1 = 0$ we can easily determine the parameter t^* at which $y_b(t)$ enters the overlap region \mathbf{D} . We solve $y_b(t^*) = 1 - t^*$. Thus $t^* = t^*(b)$ is the solution of the equation

$$\sum_{k=1}^{\infty} b_{k+1} t^k = 1. \quad (12)$$

There is exactly one solution in $[0, 1]$ since the left-hand side is increasing, with value 0 at $t = 0$ and value at least one for $t = 1$. When the curve $y_b(t)$ has entered \mathbf{D} it will remain there: it cannot cross the upper border because the left-hand side does not exceed $\frac{t}{1-t}$. For a kneading sequence c with $c_1 = 1$ these calculations would be slightly more complicated. So we use symmetry and say that $t^*(c) = t^*(1-c)$ is the solution of (12) with $b_k = 1 - c_k$.

Now consider an itinerary c which is not a kneading sequence. Then $t^*(c)$ is defined as the smallest value $t > \frac{1}{2}$ for which the G -orbit of $y_c(t)$ intersects the overlap interval D . The address curves of different points of this orbit cannot intersect for $t < t^*(c)$ since this would contradict Proposition 8. Thus, since all address curves are continuous, even smooth, the address curve of the kneading sequence b of c will be the first member of the orbit which enters \mathbf{D} , and we calculate $t^*(c) = t^*(b)$ from the kneading sequence b .

For any itinerary, $t^*(c)$ marks the right endpoint of the dark curve $y_c(t)$ in Figures 2 and 7. At the same parameter where the curve $y_b(t)$ of the kneading sequence $b = .b_1b_2\dots$ enters \mathbf{D} , the address curves of a corresponding itinerary $c = .w_1\dots w_nb_1b_2\dots$ will enter the horn $\mathbf{D}_{w_1\dots w_n}$. At this point the properties of all these curves will change: as soon as the orbit under G intersects \mathbf{D} , we have multivalued dynamics.

Binary notation assigns rational numbers to eventually periodic 01-sequences, a method used to denote external angles of the Mandelbrot set [37]. The curves $y(t)$ and $z(t)$ in (9), for instance, coincide with $y_{1/3}(t)$ and $y_{2/3}(t)$ defined above. Other rational functions of the form $y_b(t)$ are given in (10), for $b = \frac{1}{5}, \frac{2}{5}, \frac{3}{5}, \frac{4}{5}$ as is easy to check.

In the context of real unimodal maps, like the quadratic family $q_r(x) = rx(1-x)$, itineraries are the addresses of points, and kneading sequences are those addresses which for some parameter r belong to the critical point. A 01-sequence addresses different points in different maps, but in a well-behaved parametric family it can address the critical point only once, and then it disappears [36, 11]. We adapted the Milnor-Thurston notation to Bernoulli convolutions since the situation is similar. Itineraries are unique addresses of certain points, describing the b -quantiles as explained below. At the point t^* they become critical which means that the kneading sequence addresses a boundary point of \mathbf{D} , and the address curves of other itineraries enter other horns. At t^* the points cease to have a unique address and maximal local dimension. As we shall see, the curves $y_b(t)$ remain important beyond t^* although in Figures 2 and 7, $y_b(t^*)$ seems to be their endpoint.

Milnor and Thurston [36] also introduced kneading functions similar to our address curves in order to determine the topological entropy of unimodal maps. The standardizing factor $\frac{1-t}{t}$ in (11) comes from our choice of mappings g_0, g_1 which define all measures on $[0, 1]$. The following theorem says that the address curves of itineraries are just the parallel dark curves in Figures 2 and 7.

Theorem 9 (*Points with unique address, kneading functions and quantile curves*)

- (i) For each $t \in (\frac{1}{2}, t_2)$, the set A_t of points with unique address agrees with all values $y_c(t)$ outside \mathbf{D} . More exactly,

$$A_t = \{y_c(t) \mid c \text{ itinerary and } t < t^*(c), \\ \text{or } t = t^*(c), \text{ and the } g\text{-orbit of } c \text{ does not contain the kneading sequence}\}.$$

- (ii) For each itinerary $b = .b_1b_2\dots$, the kneading function $y_b(t)$ represents the b -quantile of all Bernoulli measures ν_t with $t \leq t^*(b)$:

$$F_t(y_b(t)) = \nu_t[0, y_b(t)] = b \quad \text{for } \frac{1}{2} \leq t \leq t^*(b).$$

Proof of (i). We fix some $t < t_2$ and consider the branching dynamical system G for this t . Take any itinerary c with $t < t^*(c)$. By the definition of t^* the G -orbit of $y_c(t)$ does not hit the overlap interval D . This also holds in the other case $t = t^*(c)$ by Proposition 8 since then the kneading sequences correspond to the endpoints of D . Thus $y_c(t)$ has a unique address and belongs to A_t .

To show the reverse inclusion, take a point $x \in A_t$, and let $c_1c_2\dots$ denote its unique address, explained in Section 6. Thus there is only one G -successor of x in each generation: $x_1 = g_{c_1}(x), x_2 = g_{c_2}(x_1), \dots$ In other words, the G -orbit of x does not hit $D = [1-t, t]$. By Proposition 8, the orbit of $c = .c_1c_2\dots$ under the doubling map does not hit the interval $[s, 1-s]$ where $s = \nu_t[0, 1-t] < \frac{1}{2}$. Thus c is an itinerary and $x = y_c(t)$. Moreover, $t \leq t^*(c)$ since the G -orbit of x does not hit D .

If the g -orbit of the binary number c contains a corresponding kneading sequence b then by Proposition 8 and the definition of t^* we have $t < t^*(c)$. This holds in particular for all eventually periodic sequences c , the case which is our main interest here. However, if the g -orbit of c does not contain a corresponding kneading sequence, $t = t^*(c)$ is possible. \square

Example. Let $c = 01\ 0110\ 01101001\dots$ be the concatenation of approximating words of the Morse-Thue sequence. Then $t^* = t_{KL}$ is the Komornik-Loreti point, and b is the Thue-Morse sequence which for this parameter is an address of the endpoint $1 - t^*$ of D which has $1\bar{0}$ as second address. However $y_c(t^*)$ has only the address c . Taking $c = (01)^{k_1}(0110)^{k_2}(01101001)^{k_3}\dots$ with nonnegative integers k_i we obtain uncountably many sequences with the same properties.

Our address curves are analytic functions for $0 < t < 1$. The assertion that points with unique address come on smooth curves seems to be new. We consider address curves as structural elements of the Bernoulli scenario which provide a smooth pattern at least outside **D**. A consequence of (i) is that

$$A_t \subseteq \overline{A_t} \subseteq \{y_c(t) \mid c \text{ itinerary and } t \leq t^*(c)\} =: \tilde{A}_t,$$

and all three sets coincide if the G -orbits of t and $1 - t$ hit the interior of D , as for instance for $t \in (s_2, t_2)$. If the orbit of $1 - t$ avoids the interior of D (and so has either two or countably many addresses), the sets differ by a countable set of preimages $f_w(t), f_w(1 - t)$ outside D . In this case $1 - t$ can be an accumulation point of A_t , as in the above example. Then $\overline{A_t} = \tilde{A}_t$ and the difference occurs between the closure $\overline{A_t}$ and A_t . When $1 - t$ is not an accumulation point, as for $t = t_2$, then A_t is closed and $\tilde{A}_t \setminus A_t$ is countable. The differences often do not matter, for instance in calculating Hausdorff dimension or measures.

8 Geometry of itineraries and kneading sequences

The topological structure of A_t is the subject of a comprehensive paper by de Vries and Komornik [14] based on properties of greedy and quasi-greedy β -expansions. It collects earlier results of several authors and considers the general case $\beta > 1$. In [23, 14, 44], $\mathcal{U}_q, \mathcal{V}_q$ denote the non-standardized version of A_t, \tilde{A}_t , and q means β .

The goal of this section is to give a direct self-contained, geometric and dynamic view of the A_t , for our case $1 < \beta \leq 2$, to prove (ii) of Theorem 9 and indicate connections with one-dimensional dynamics. Roughly speaking, all combinatorial and topological questions boil down to the study of the angle-doubling map. For $m - 1 < \beta \leq m$ with $m > 2$ we would have to take the map $mx \bmod 1$.

To each set A_t we can assign the set I_t of initial points $y_c(\frac{1}{2})$ of the curves y_c with $y_c(t) \in A_t$. Assertion (ii) says that F_t maps A_t to I_t . Note that F_t is a homeomorphism on $[0, 1]$ since the measure ν_t has no point masses, and each interval has positive measure. This suggests that the study of the sets \tilde{A}_t can be replaced by the study of sets S_b of binary itineraries subordinated to a given kneading sequence b . The S_b have a rather simple structure. In the following statement $f_0(x) = x/2, f_1(x) = (x + 1)/2$, and f_w for a 01-word w is the corresponding composition of mappings, as explained in Section 6.

Proposition 10 (Structure of itineraries subordinated to a kneading sequence)

Let $b < \frac{1}{2}$ be a kneading sequence and $J = (b, 1 - b)$. Let S_b be the set of all itineraries for which the orbit under the doubling map does not meet J . Then there is a set W of 01-words such that the intervals $J_w = f_w(J)$ with $w \in W$ are pairwise disjoint, and

$$[0, 1] \setminus S_b = \bigcup_{w \in W} J_w.$$

Actually, W consists of all words $w = w_1\dots w_m$ such that for $k = 1, \dots, m - 1$ the binary number $.w_k\dots w_m$ is not in the interval $[b, 1 - b)$. Moreover, b is either an isolated point of S_b ,

or an accumulation point of the points $f_w(b)$ with $w \in W$. The first case happens if and only if b is a periodic binary number of the form $.w(1-w)$.

Proof. First we show that the intervals $J_v = f_v(J)$ for all 01-words form a nested sequence: any two of them are either disjoint, or one is contained in the other. Namely, if J_v would contain an endpoint of J , for some word v of length $n > 0$, then $g^n(b)$ or $g^n(1-b)$ would be in the interior of J which cannot happen since b and $1-b$ are kneading sequences. Next, if J_u contains an endpoint of J_v , but not the whole set J_v for some words $u = u_1 \dots u_m$ and $v = v_1 \dots v_n$ then we must have $u_1 = v_1$ since $f_0(0,1) \cap f_1(0,1) = \emptyset$, and $J_{u_2 \dots u_m}$ and $J_{v_2 \dots v_n}$ satisfy the same overlap relation as J_u and J_v . Repeating this argument we come to the case where one of the intervals is J , which was shown to be impossible.

Thus the J_v are nested, and we let W be the set of words w for which J_w is not contained in any other J_v . Note that an itinerary $c \in S_b$ cannot be in any J_v , and any point outside the union of all J_v must be an itinerary. Thus $\bigcup_{w \in W} J_w$ is the complement of S_b . The inductive argument above says that $J_u \subset J_v$ for $u = u_1 \dots u_m$ and $v = v_1 \dots v_n$ if and only if $m > n$ and $u_i = v_i$ for $i = 1, \dots, n$ and $J_{u_{n+1} \dots u_m} \subset J$. The characterization of $w \in W$ says that this cannot happen.

b is isolated if it is the right endpoint of an interval J_w for some nonempty word $w \in W$. Thus $b = f_w(1-b)$, and by symmetry $1-b = f_{1-w}(b)$, consequently $b = f_w f_{1-w}(b)$. Otherwise, every interval $(b-\epsilon, b)$ with $\epsilon > 0$ contains an interval J_w with $w \in W$, and $f_w(b)$ is the left endpoint of that interval. \square

Remarks. (Structure and Hausdorff dimension of A_t)

1. The condition for W allows to determine the number a_m of holes J_w in the Cantor set S_b on every level m , and the growth rate $\rho = \lim_{m \rightarrow \infty} \frac{\log a_m}{m}$. The Hausdorff dimension of S_b then is $\log \rho / \log 2$, cf. Kong and Li [32].
2. The above proof works for the sets A_{t^*} with $t^* = t^*(b)$ when we replace J by $(1-t^*, t^*)$. It is also possible to relate S_b to A_{t^*} by assigning to each starting point $(\frac{1}{2}, c)$ of a blue curve with $c \in S_b$ the terminal point $(t^*, y_c(t^*)) = (t^*, 1-t^*)$ with $t^* = t^*(b)$. Thus A_{t^*} has the same similarity structure with mappings of contraction factor t as S_b with contraction factor $\frac{1}{2}$. As a consequence [32, Theorem 2.6], for $t = t^*$

$$\dim A_t = \frac{\log \rho}{-\log t} = \frac{\log \rho}{\log \beta} \quad (13)$$

3. In the case where b is isolated, ρ can be determined explicitly, similar to Proposition 3, cf. [13, 30]. In particular, when W consists of all words which do not have k consecutive equal symbols, for some $k \geq 3$, then $\rho = t_{k-1}$. This holds for $b = (2^{k-1} - 1)/(2^k - 1)$ and $t^*(b) = t_k$, and was used in [29, 23] to show $\dim A_t \rightarrow 1$ for $t \rightarrow \frac{1}{2}$.
4. The S_b form an increasing sequence, so their dimension increases with b . However, Kong and Li [32] observed that $\dim A_t$ *sometimes decreases* with decreasing t . When b is periodic, there is an interval (b, b') which does not contain kneading sequences, see Proposition 11 below. For $t \in (t^*(b'), t^*(b))$ the above proof, with $(1-t, t)$ instead of J , still yields equation (13), and A_t has the same similarity structure while $\log \beta$ increases with decreasing t . On such intervals, $\dim A_t$ smoothly decreases with decreasing t .

Let us now study the structure of the set K of all kneading sequences $b < \frac{1}{2}$. In Figure 7, kneading sequences are represented as endpoints of blue curves on the line $y = 1-t$.

To any starting point $(\frac{1}{2}, b)$ for a kneading sequence $b < \frac{1}{2}$ we assign the 'terminal' point $(t^*, y_b(t^*)) = (t^*, 1 - t^*)$ with $t^* = t^*(b)$. However, many blue curves correspond to itineraries which are not kneading sequences. The set A_{t^*} is the intersection of the vertical line $t = t^*$ with all blue curves. Going back on the curves, we get the corresponding set S_b on the vertical line $t = \frac{1}{2}$.

Figure 8 shows only the address curves of $b \in K$, except for $b = \frac{1}{3}$ which is outside range. Each kneading sequence is represented by the intersection of its address curve with $y = 1 - t$, and curves are extended up to the line $y = \frac{1}{2}$ where some of them meet. The points $(t^*, 1 - t^*)$, as well as the kneading sequences b on the left axes, form a Cantor set plus a sequence of isolated points in each cutout interval which always converges to the left endpoint of the interval, which is a Komornik-Loreti point. This phenomenon is well-known from one-dimensional dynamics, where the 'bifurcation points' form a geometric sequence studied by Feigenbaum and others, and so are better visible due to the slowdown of the dynamics when the parameter reaches a Feigenbaum point. In Figure 8 we use binary words to denote the periodic windows of the Feigenbaum diagram, which corresponds to the notation of the Mandelbrot set [37], not to the original Milnor-Thurston addressing. With this notation, the correspondence between parameter windows with stable periodic orbit, and gaps in the Cantor set of kneading sequences is one-to-one. In the lower picture, however, the distance of isolated points to the left endpoint of the gap interval decreases with order t^{2^n} , that is, with double exponential speed, so that only the very first isolated kneading sequences can be distinguished from the corresponding Komornik-Loreti limit. Compare Figure 7 for the basic case $.0\overline{1}$, $.0\overline{110}$, ... with $t^* = t_2, s_2, \dots \rightarrow t_{KL}$, and the thick black lines in Figure 9 for $.0\overline{11} = 3/7$ with $t^* = t_3$, $.0\overline{11100} = 4/9$ with $t^* = s_3$, and $.0\overline{11100100011} = 607/1365$.

Remark. (Potential of correspondence between quadratic maps and β -expansions)

There is a vast literature on the dynamics of real unimodal maps. Some results carry over to β -expansions and Bernoulli convolutions. One instance is Sharkovskii ordering of orbit lengths of real continuous maps which was proved to hold for the dynamics of G on the A_t by Allouche, Clarke, and Sidorov [2]. The existence of absolutely continuous invariant measures is a central problem in one-dimensional dynamics, and Misiurewicz parameters play a similar part as Garsia numbers here. Sometimes the setting of linear expansive maps is simpler than quadratic maps: a point of period n is a root of a polynomial of degree n while for quadratic maps the degree would be 2^n .

The following well-known fact explains the period-doubling sequences of isolated kneading addresses. It says that every periodic sequence $b \in K$ is isolated from the left in K , and if it has the form $b = .\overline{w(1-w)}$ for some word w , it is also isolated from the right. See [4, Section 3] for related facts references.

Proposition 11 (Period-doubling lemma)

Let $b = .\overline{0b_2\dots b_n}$ be a periodic kneading sequence. There is no kneading sequence between b and $b' = .\overline{0b_2\dots b_n1(1-b_2)\dots(1-b_n)}$.

Proof. Let $c > b$ be a kneading sequence which we try to make as small as possible. Let k be the first index for which $c_k > b_k$. For $k > n+1$ the sequence c would not be kneading, so we take $k = n+1, c_{n+1} = 1$. Since $.c_{n+1}c_{n+2}\dots \geq 1 - c = .1(1-b_2)\dots(1-b_n)0\dots$ we inductively conclude $c_{n+j} \geq 1 - c_j$ for $j = 2, 3, \dots$ and take $c_{n+j} = 1 - c_j$ as optimal choice. This yields $c = b'$. Since b is a kneading sequence, b' also fulfils this condition. \square

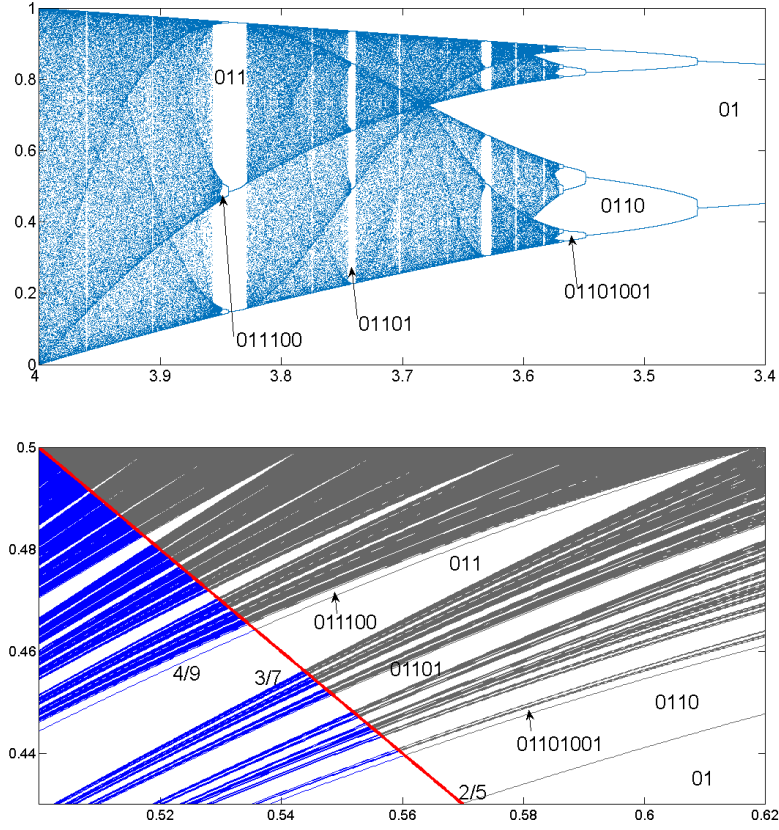


Figure 8: Bifurcation diagram of the quadratic family $q(x) = rx(1-x)$, $r \in [3.4, 4]$ with binary itineraries for 'periodic windows' [11, 36, 37], and address curves of kneading sequences in our scenario. Combinatorial structures coincide while metric structures differ a lot. In the lower panel, intersection with the line $y = 1 - t$ represents kneading sequences, and univoque numbers as a subset.

A number $\beta \in (1, 2)$ is called *univoque* if the equation

$$\sum_{k=1}^{\infty} c_k \beta^{-k} = 1 \quad \text{with coefficients} \quad c_k \in \{0, 1\} \quad (14)$$

has only one solution. This concept was thoroughly studied in connection with β -expansions [16, 12, 13, 4, 14]. A basic fact is that *the set of univoque representations agrees with the set of non-periodic kneading sequences* [16, Theorem 1], [4, Theorem 2.3]. Thus univoque parameters $t = 1/\beta$ are obtained by removing all isolated points and right endpoints of gaps from K , considered as set of $t^*(b)$. This implies the topological statements in [14], where the sets are denoted \mathcal{U}, \mathcal{V} . In particular, the set of univoque numbers is not compact.

Proposition 12 (Univoque numbers and kneading sequences [16], Theorem 1)

Let $\beta \in (1, 2)$ and $c_1 c_2 \dots$ a 01-sequence which fulfil (14). Then β is univoque if and only if $b = .0c_1 c_2 \dots$ is a non-periodic kneading sequence. If this is true, $\beta = 1/t^*(b)$, that is, β is determined by (14).

Proof. If β is univoque with coefficients c_k , and $b = .0c_1c_2\dots$ then $y_b(t) = 1 - t$ by definition. b is a kneading sequence and $t = t^*(b)$ since the G -orbit of $1 - t$ does not meet D , by the univoque condition. The assumption of periodic $b = .\overline{0c_1\dots c_k}$ implies

$$1 - t = y_b(t) = \frac{1 - t}{1 - t^{k+1}} \sum_{j=1}^k c_j t^j \quad \text{and} \quad t^{k+1} + \sum_{j=1}^k c_j t^j = 1 ,$$

which contradicts the univoque assumption. So b is non-periodic.

Conversely, for a non-periodic kneading sequence $b < \frac{1}{2}$ and $t = t^*(b)$ the G -orbit of $1 - t$ will never return to D . So $1 - t$ has only two addresses $b = .0b_2b_3\dots$ and $.1\bar{0}$. This implies that b_2, b_3, \dots is the only possible coefficient sequence for the representation of 1 , and β is univoque. \square

Univoque Pisot numbers were studied by Allouche, Frougny and Hare [4] for which Theorem 5 says that b must be eventually periodic. Thus a Pisot number is univoque if and only if b is preperiodic. An extensive, partly computer-assisted search in [4] proved that the preperiodic case is quite rare for Pisot numbers:

Theorem 13 (Smallest univoque Pisot numbers [4])

The smallest accumulation point of univoque Pisot numbers is the root $\chi \approx 1.9052$, $t \approx .5256$ of $x^4 - x^3 - 2x^2 + 1$. This is the only accumulation point of Pisot numbers with preperiodic kneading sequence. Only two univoque Pisot numbers are below χ , at 1.8800 and 1.8868. \square

The address of χ is $.011\bar{1}\bar{0} = \frac{11}{24}$. It will show up at Theorem 18 below. The following approximation of kneading sequences by periodic ones will be needed in the proof below.

Proposition 14 (Approximation of kneading sequences by periodic ones)

Let $b = .b_1b_2\dots < \frac{1}{2}$ be a nonperiodic kneading sequence and $J = (b, 1 - b)$. The orbit of $s_n = .\overline{b_1\dots b_n}$ under the doubling map does not meet J if $b_{n+1} = 1$ and there is no $k < n$ such that $(1 - b_k)\dots(1 - b_{n+1}) = b_1\dots b_{n-k+2}$. There are infinitely many n with this property.

Proof. $b_{n+1} = 1$ implies $s_n < b$, and $g^m(s_n) < g^m(b) \leq b$ whenever $b_{m+1} = 0$ and $1 \leq m \leq n$. Thus $g^m(s_n)$ cannot belong to $(b, \frac{1}{2}]$ for any $m \geq 1$. Now suppose that $g^m(s_n) \in (\frac{1}{2}, 1 - b)$ for some $m < n$. Then $b_{m+1} = 1$ and $.b_{m+1}\dots b_n 0 < 1 - b$ while $.b_{m+1}\dots b_n b_{n+1}\dots \geq 1 - b$ holds because b is a kneading sequence. Hence $.(1 - b_{m+1})\dots(1 - b_n)1 > b$ and $.(1 - b_{m+1})\dots(1 - b_n)0 \leq b$. So this last word must be a prefix of b which contradicts the assumption. The first statement is proved.

Induction will show that the assumption is fulfilled for infinitely many n . Suppose that at some stage, we have problems to find the next n since there is a word $b_k b_{k+1}\dots$ which is the complement of a prefix of b . The word cannot extend to infinity because then b would be periodic, with period $2(k - 1)$. Take the smallest m such that $(1 - b_k)\dots(1 - b_m)$ is a prefix of b but $1 - b_{m+1} \neq b_{m+2-k}$. By the kneading property, $b_{m+1} = 1 = b_{m+2-k}$. There can be no $k' > k$ such that $(1 - b_{k'})\dots(1 - b_m)0$ is a prefix of b since $(1 - b_{k'})\dots(1 - b_m)1$ is a subword of b whenever $k \leq k' < m$. We found the next $n = m$ and can continue. \square

Proof of Theorem 9, (ii). Consider first an eventually periodic 01-sequence $b_1b_2\dots$. It is an itinerary if it does not end with $\bar{0}$ or $\bar{1}$. The corresponding binary number $b = .b_1b_2\dots$ is rational but not of the form $k/2^n$. So the orbit under g is finite and Proposition 2 applies. We obtain all values $F_{\frac{1}{2}}(g^k(b))$ from the equations of the Markov partition. Of course we know that $F_{\frac{1}{2}}(x) = x$ since $\nu_{\frac{1}{2}}$ is the uniform distribution. However, Proposition 8 says that

for $t < t^*(b)$ the orbit of $y_b(t)$ is also finite, and gives rise to exactly the same equations for the Markov partition. In particular $F_t(y_b(t)) = F_{\frac{1}{2}}(b) = b$. It is easy to see that this is also true for $t = t^*(b)$ since Bernoulli convolutions have no point masses.

Next, we prove (ii) for nonperiodic kneading sequences b . Proposition 14 says that the binary number $b = .b_1b_2\dots$ can be approximated by periodic sequences s_n with $t^*(s_n) \geq t^*(b)$. So the address curves $y_{s_n}(t)$ converge to $y_b(t)$ for $\frac{1}{2} \leq t \leq t^*(b)$. Since (ii) holds for the s_n and the ν_t are nonatomic measures, (ii) must hold for b .

Now we show (ii) for itineraries. Suppose b is an itinerary with $F_t(y_b(t)) = b$ and $t \leq t^*(b)$, and $c = b/2$ is also an itinerary with $t^*(c) = t^*(b)$. Then $y_c(t) = t \cdot y_b(t)$ by definition, and Proposition 8 implies $F_t(y_c(t)) = b/2 = c$ since

$$2F_t(y_c(t)) = F_t \cdot g_0(y_c(t)) = F_t(y_b(t)) = b.$$

A similar equation holds when $c = (b+1)/2$ is an itinerary. By recursion, (ii) is carried over from a kneading sequence b to all itineraries d with $t^*(d) = t^*(b)$ which have b in their G -orbit. Proposition 10 says that such points d approximate also the other itineraries which have b only in the closure of their G -orbit. So (ii) holds for them since F_t is a homeomorphism. \square

The quantile property (ii) directly implies that address curves cannot intersect at $t < t^*$, that is, outside the horns \mathbf{D}_w . It gives some information on ν_t for all $t \leq t_2$, no matter whether singular or absolutely continuous. Moreover, for periodic or preperiodic binary numbers b the address curve is a rational function of t .

This also holds for $b = .b_1b_2\dots b_m\overline{10}$ which is not an itinerary. In this case, $y_b(t)$ is the middle curve of the horn \mathbf{D}_w with $w = b_1\dots b_m$ which is mapped by g_w onto the middle curve $y = \frac{1}{2}$ of \mathbf{D} . As long as these curves enter no horns of lower level, they also represent the b -quantile of all ν_t . For example, the curve $y(t) = \frac{t}{2}$ in the middle of \mathbf{D}_0 represents the $\frac{1}{4}$ -quantile for all $t \leq \frac{2}{3}$ where $y(t)$ hits the lower border $1 - t$ of \mathbf{D} . For \mathbf{D}_{01} the equation $\beta^2 y + 1 - \beta = \frac{1}{2}$ leads to the middle curve $y(t) = t - \frac{1}{2}t^2$ which defines the $\frac{3}{8}$ -quantile for $t \leq 2 - \sqrt{2}$. The general case is proved by induction and (1). In contrast to other quantile curves, the density of ν on these curves is not zero.

9 Density zero inside the overlap region

The single-valued dynamics of G outside D is the easy part. We saw that it boils down to the doubling map. The multi-valued dynamics inside D is much less understood. Our view is that the address curves remain structural elements within \mathbf{D} , and their intersections determine zeros and poles of the two-dimensional density Φ .

We start with a look on Figure 9. Some address curves have been extended beyond the parameter t^* where they enter \mathbf{D} . As mentioned above, the three thick curves in the lower part correspond to the period 3 doubling scenario starting with $\overline{.011} = 3/7 \approx .429$. The period 4 doubling scenario is represented by the addresses $\overline{.0111} = 7/15 \approx .467$ and $\overline{.01111000} = 8/17 \approx .471$ and by their counterparts $\overline{.1000} = 8/15$ and $\overline{.10000111} = 9/17$ which come from above. Period 5 doubling is represented only by two curves with $b > \frac{1}{2}$, namely $\overline{.10000} = 16/31$ and $\overline{.1000001111} = 529/1023$. Each number denotes the starting point of the respective curve at $t = \frac{1}{2}$ which is not visible in the figure.

The two thin lines without numbers arise as images under f_{01} of the $7/15$ and $8/15$ curve. Their addresses are preperiodic, $\overline{.010111} = 22/60 \approx .367$ and $\overline{.011000} = 23/60 \approx .383$. Finally, there are two dashed lines with preperiodic addresses $\overline{.011100} = 9/20 = .45$ and $\overline{.01110} = 11/24 \approx .458$, and these curves pass through regions with small Φ -values, which

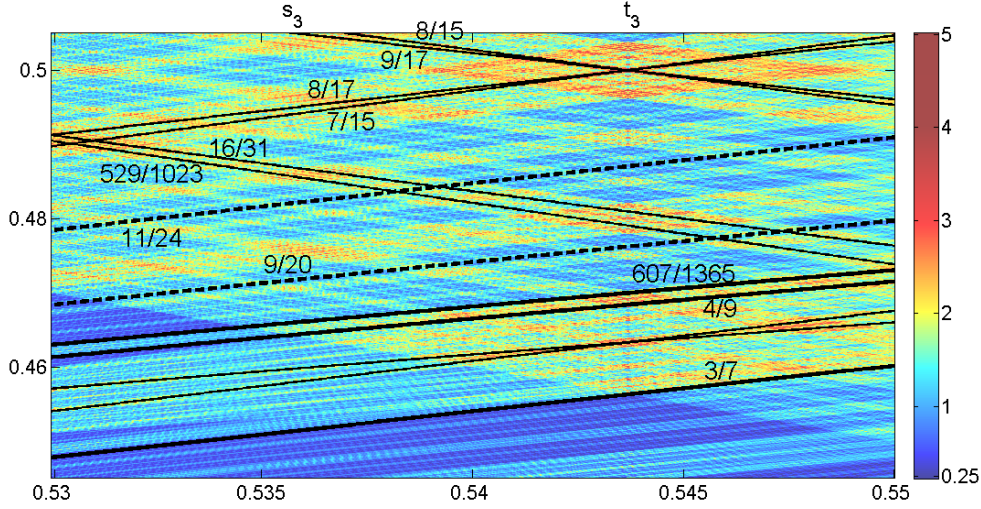


Figure 9: A magnification of Figure 7 near the tribonacci parameter t_3 . Address curves of some eventually periodic itineraries are shown in black and extended into the overlap region.

will be proved rigorously. The periodic address curves, however, pass through high Φ -values, at least at those places where such curves intersect.

Since the addresses are eventually periodic, the curves are rational functions of t . So the t -value of an intersection point of two such curves is a root of a polynomial, and $\beta = 1/t$ is a Perron number according to Theorem 7. All curves of the period 4 doubling scenario intersect at $(t_3, \frac{1}{2})$, and the period 3 curves meet at $(t_2, \frac{1}{2})$, as can be seen in Figure 8. A similar fact can be checked for period n and the multinacci parameter t_n . Actually, all other periodic kneading sequences, like $\overline{01101}$ give rise to a doubling scenario with infinitely many address curves which will all meet at a point $(t, \frac{1}{2})$ where $\beta = 1/t$ is a Perron number.

Intersections of periodic address curves $y_b(t), y_c(t)$ will be treated in the next section. Here we consider those intersections which give small Φ values. When b and c have a common prefix, say $b = ab'$ and $c = ac'$ with $a = a_1 \dots a_n$, then $y_{b'}(t)$ and $y_{c'}(t)$ will intersect at the same parameter(s) t as $y_b(t)$ and $y_c(t)$, and the y -coordinate of the latter intersection point is in the G -orbit of the former. For this reason we shall assume $b_1 \neq c_1$.

Proposition 15 (Intersection points with two addresses)

Let b, c be nonperiodic kneading sequences with $b_1 = 0$ and $c_1 = 1$, let $t \in (\frac{1}{2}, t_2]$ be the smallest parameter for which $y_b(t) = y_c(t) = y$, and suppose the G -orbit of y does not return to D . Then y has exactly two addresses, the local dimension of ν_t at y assumes its maximal value $\log 2 / \log \beta$, and the density of ν_t at y is zero. All points in D with two addresses are obtained in this way.

Proof. The assumption implies that y is in D , and both $g_0(y)$ and $g_1(y)$ have unique addresses. The value of the dimension comes from Proposition 4. \square

Figure 10 indicates that this case happens very often when $t < t_3$. Points with two addresses seem to form Cantor carpets within \mathbf{D} . For $b > 0.469$, the binary sequence starts $b = .01111b_6\dots$ so that $y_b(t) = (1-t)(t+t^2+t^3+t^4+\dots) = t-t^5+\dots$. Thus near $t = \frac{1}{2}$, the curves $y_b(t)$ become parallel to the line $y = t$, and the curves $y_c(t)$ become parallel to

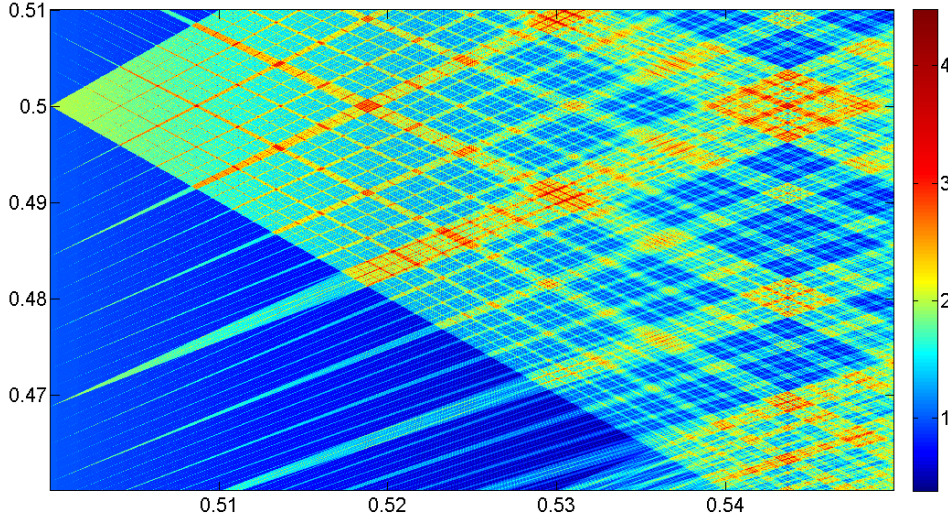


Figure 10: Near $t = \frac{1}{2}$ the structure of Φ looks self-similar, with lots of zeros within \mathbf{D} . Landmark parameters are the multinacci numbers t_n , the doubling numbers s_n , and other Perron parameters.

$y = 1 - t$. A better explanation of the apparent product structure of the dark carpets within \mathbf{D} is an observation of Sidorov [44, Lemma 2.2] which we reformulate for our setting.

Proposition 16 (Condition for points with two addresses)

For fixed $t < t_2$, there is a one-to-one correspondence between points $y \in D$ with exactly two addresses and pairs of points $x, x' \in A_t$ with $x - x' = \beta - 1$. In particular, points with two addresses exist if and only if $\beta - 1$ belongs to the difference set $A_t - A_t$.

Proof. Given y , we let $x = g_0(y)$ and $x' = g_1(y)$. Given x, x' let $y = f_0(x) = f_1(x')$. \square

Since $\beta - 1 > 1 - t$ for $0 < t < 1$, we must always have $x > \frac{1}{2}$ and $x' < \frac{1}{2}$. Thus we can construct the g_1 -image of the points with two addresses as

$$\text{intersection of } \{x' \in A_t \mid x' < \tfrac{1}{2}\} \quad \text{with} \quad \{x + 1 - \beta \mid x \in A_t, x > \tfrac{1}{2}\}. \quad (15)$$

Using address curves, this can be done for all $t < t_2$ together. This explains the Cantor product structure, but it does not clarify how large the set of points with two addresses is for fixed t . The best answer to this question for t near $\frac{1}{2}$ was found by Sidorov.

Theorem 17 (Points with two addresses for all $t < t_3$ [44], Theorem 4.2)

For each $t < t_3$, there is at least one point with exactly two addresses. \square

As Figure 11 shows, (15) can be easily applied to $s_2 < t < t_2$ where A_t is given only by the itineraries $2^{-k}\frac{1}{3} = .0^k\overline{01}$ and $1 - 2^{-k}\frac{1}{3} = .1^k\overline{10}$ for $k = 0, 1, 2, \dots$. The shifted curve of $2/3$ is out of range, and only $k \leq 4$ is considered. The curves for $k > 4$ are between $y_{1/48}$ and 0, and between $y_{47/48}$ and $2 - \beta$ so they provide no other intersection points. There are intersection points at t_2 where we have no points with unique address, and at the doubling number s_2 . The largest parameter $t \approx .5846$ admitting points with two addresses was found by Sidorov

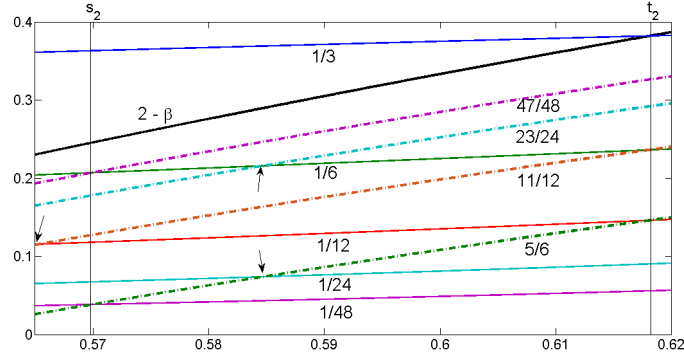


Figure 11: Points with two addresses for $0.565 \leq t \leq 0.62$ obtained by intersections of curves $x'(t), x(t)$ given in (15). The first set is represented by solid lines, the second by dotted ones.

[44, Proposition 2.4]. Figure 11 demonstrates that this is the only parameter $t > s_2$ with this property [44, Theorem 2.8]. The intersection points are marked by two arrows.

Figure 11 shows another intersection parameter $t < s_2$ at the left border, marked by a single arrow. In this case, $x = 1 - x'$, so for symmetry reasons the point with two addresses must be $y(t) = \frac{1}{2}$. We have $x'(t) = t^3/(1+t)$ with address $.000\bar{1}$ and $y = f_1(x')$ with address $b = .1000\bar{1}$. Curiously, $1/t^*(b)$ is the Pisot number χ of Theorem 13. The equation $y(t) = t^4/(1+t) + 1 - t = \frac{1}{2}$ with $t \neq 1$ yields $2t^2(t+1) = 1$ and $t \approx .5652$, a Garsia parameter:

Theorem 18 (Parameters for which $\frac{1}{2}$ has only two addresses)

There are uncountably many parameters t for which the central point $\frac{1}{2}$ has exactly two addresses. The parameter $t = 1/\beta \approx .5652$, where β denotes the real root of $x^3 - 2x - 2$, is the largest accumulation point of this set. The largest isolated parameter is $t \approx .5674$.

Proof. Due to symmetry, Proposition 16 simplifies for the central point: $y = \frac{1}{2}$ admits exactly two addresses if and only if $y + \frac{1-\beta}{2} = 1 - \frac{1}{2t} =: \varphi(t)$ belongs to A_t . Let $\psi(t) = t^3(1-t)$ denote the lower bound of the horn $\mathbf{D}_{000} = f_{000}(\mathbf{D})$ with tip at $t = \frac{1}{2}, y = \frac{1}{16}$ (cf. Figure 6). We have $\varphi(0.5) = 0 < \psi(0.5) = 1/16$ and $\varphi(0.54) \approx .0741 > \psi(0.54) \approx .0724$ so all address curves of itineraries $c < 1/16$ with $t^*(c) \geq 0.54$ will intersect the curve $\varphi(t)$ on the interval $[0.5, 0.54]$. There are uncountably many kneading sequences $b < \frac{1}{2}$ with $t^*(b) \geq 0.54$, and for each of them $c = 000b$ is an appropriate itinerary.

As shown above, $t \approx .5652$ marks the intersection point of $\varphi(t)$ with $y_{000\bar{1}}(t)$. Now $\varphi(t)$ is strictly increasing, and for $t < s_2 \approx .5698$ the address curves of $00(01)^n 0\bar{1}1\bar{0}$ approximate $y_{000\bar{1}}(t)$ from above, as noted after (10). So $\varphi(t)$ must intersect almost all of these curves. Calculation shows that the largest intersection point below s_2 appears for $n = 3$ at $t \approx .5674$. Other address curves need not be considered since $t^*(.0110100\bar{1}) \approx .5604$. \square

Theorem 18 is somewhat surprising since at first glance one would expect that Bernoulli convolutions cannot have density zero at the center of the interval. It also answers a question in [44, Section 5]: Let \mathcal{B}_m denote the set of parameters t which admit points with exactly m addresses. Consider the set of $\mathcal{B}_2 \cap [t_{KL}, t_2]$. Is this set discrete? No, it has accumulation points. An argument similar to the proof above shows that s_2 is an accumulation point of the set from the left, using address curves of $0^3(01)^n 0\bar{0}1\bar{1}$ approaching $y_{1/48} = y_{0^3 0\bar{1}}$ in the lower left corner of Figure 11. Hence s_2 is the largest accumulation point of this set.

The sets \mathcal{B}_m for $m > 2$ are obviously subsets of \mathcal{B}_2 . They were studied in [44, 7] and will not be treated here. The set \mathcal{B}_{\aleph_0} of parameters admitting points with infinite countable number of addresses, however, is not a subset of \mathcal{B}_2 . Such parameters can be generated similar to Proposition 16.

Proposition 19 (Intersection points with countable number of addresses)

Let b be a nonperiodic and c a periodic kneading sequence with $b_1 \neq c_1$, let $t \in (\frac{1}{2}, t_2]$ be the smallest parameter for which $y_b(t) = y_c(t) = y$, and suppose the G -orbit of y does not return to $D \setminus \{y\}$. Then y has a countably infinite number of addresses, the local dimension of ν_t at y assumes its maximal value $\log 2 / \log \beta$, and the density of ν_t at y is zero.

Proof. If $b = b_1 b_2 \dots$ and $c = \overline{w}$ with $w = c_1 \dots c_n$, the addresses of y have the form $w^k b$ with $k = 0, 1, 2, \dots$ \square

We briefly study the interval $t_{KL} < t \leq t_2$ where all points of A_t are eventually periodic. For such parameters t , points with two addresses arise iff two preperiodic address curves meet. Points with countably many addresses arise when a periodic kneading sequence meets a preperiodic one, or, perhaps, infinitely many preperiodic curves meet in one point. Theorem 7 applies to all these cases, which improves [44, Theorem 2.1]:

Proposition 20 (Number of addresses within first doubling scenario)

If $t_{KL} < t \leq t_2$ and $\beta = 1/t$ is not a weak Perron number, then each point y has either one address or uncountably many addresses.

In contrast to \mathcal{B}_2 , the set \mathcal{B}_{\aleph_0} includes t_2 , and every other t for which $1 - t$ has a periodic address $b = .\overline{0b_2 \dots b_n}$ which is a kneading sequence. These were the non-univoque numbers excluded in Proposition 12.

We conclude the section with two examples near t_2 . Proposition 19 applies to the kneading sequences $b = \frac{5}{12} = .01\overline{10}$ and $c = 8/15 = .\overline{1000}$, with intersection parameter $t \approx .5951$ and $y \approx .463$. For $c' = 135/255 = .\overline{10000111}$ we also get an intersection point with the address curve $y_b(t)$ at $(t', y') \approx (.6045, .4668)$. The G -orbit of y' returns to $1 - y'$ and is countable although Proposition 19 does not apply.

10 Singularities inside the overlap region

So far we studied points y which have very few addresses - a finite or countable number, while almost all points in $[0, 1]$ have an uncountable number of addresses [43, Theorem 3.6]. These points have an interesting structure but they do not cause ν_t to become singular. Now we consider points y which have network-like orbits under G , where at least two cycles in the network have a common point. The growth rate of such points is always positive, and they can have an extraordinary number of addresses:

Theorem 21 (Intersections of periodic address curves)

Let $b = .\overline{0b_2 b_3 \dots b_m}$ and $c = .\overline{1c_2 c_3 \dots c_n}$ be periodic itineraries, and let the two curves $y_b(t), y_c(t)$ intersect in the point (s, z) inside the overlap region D . Then

- (i) Infinitely many periodic address curves meet in (s, z) .
- (ii) The growth rate of the orbit of z is at least as large as the positive solution of

$$x^{-m} + x^{-n} = 1 . \quad (16)$$

- (iii) If the growth rate of the orbit of z exceeds $2s$ then ν_s does not have a bounded density. A possible density function of ν_s must be unbounded on each interval, and discontinuous at every point of $[0, 1]$.

Proof. (i) If z is the fixed point of f_v and f_w , with $v = 0b_2b_3\dots b_m$ and $w = 1c_2c_3\dots c_n$, then z is also the fixed point of f_{vw} and f_{wv} , of f_{vwwv} and f_{vvww} , of f_{vwvvww} and so on. Thus z belongs to the address curves of \overline{vw} , \overline{vwvw} etc.

(ii) We show that the growth rate of a graph containing two directed cycles of length m and n which meet in a vertex x is at least as large as the positive solution of (16). When z is the only intersection point of the cycles and there are no further edges, the number $\gamma^q = \gamma^q(z)$ of successors of z in generation q is given by the equation $\gamma^q = \gamma^{q-m} + \gamma^{q-n}$. The standard ansatz $\gamma^q = x^q$ leads to (16), and the solution is unique since we look for the spectral radius of a graph and the Perron eigenvalue is unique. When the cycles meet in other vertices and/or there are more edges in the graph, the number of successors of z can only become larger.

(iii) If ρ denotes the growth rate of z , Proposition 4 says that the local dimension is $d = d_z(\nu) = \log(2/\rho)/\log \beta$. Thus $d < 1$ if and only if $\rho > 2/\beta = 2t$. In case $d < 1$ a possible density function ϕ of ν cannot be bounded in a neighborhood of z . Since $d_{f_w(z)}(\nu) \leq d_z(\nu)$ for any 01-word w , and the points $f_w(z)$ are dense in $[0, 1]$, the function ϕ must be unbounded on each interval. This implies that ϕ is discontinuous at each $x \in [0, 1]$. \square

Remarks (Corollaries and improvements of Theorem 21)

1. For kneading sequences with $c = 1 - b$ we get in (i) the doubling scenario of Section 8. In this case $z = \frac{1}{2}$, and Figure 8 shows how the bundle of address curves, representing a gap of the set of kneading sequences, converges to a point $(s, \frac{1}{2})$ where the gap closes. Such intersection points are dense on the line $y = \frac{1}{2}$. In the theory of Milnor and Thurston [36], all unimodal maps with addresses from a doubling scenario have the same topological entropy, namely $-\log s$. This is also the case here for certain β -expansions. The formulation with words v, w is an immediate generalization, and can be related to topological entropy of Lorenz maps, which will not be done here. In the general case, the addresses need not be kneading sequences.
2. Here is a little corollary without formal proof. Imagine that $1/s$ is a Pisot number, so that intersection points z of periodic addresses are dense in D . Then the bundles of sufficiently close intersection points z_1, z_2 must intersect each other, either left or right of s . Thus a Pisot parameter is always an accumulation point of other parameters where periodic addresses meet, both from the right and from the left. Since there are only few accumulation points of Pisot numbers, most of the approximating parameters will not be Pisot, only weak Perron by Theorem 7.
3. Combining (ii) with (iii), we can say that there is no bounded density if

$$(2s)^{-m} + (2s)^{-n} > 1. \quad (17)$$

The case $m = n$ was found by Feng and Wang [21, Theorem 1.4] who also gave several conditions under which a density cannot belong to L^q for various q .

4. In general, the estimates (16) and (17) are rather weak. For a given $t_0 > \frac{1}{2}$ there can be only finitely many parameters $s > t_0$ for which these conditions are fulfilled. To see this,

assume $m \leq n$, and take m_0 so that $(2t_0)^{-m_0} < \frac{1}{2}$. Then (17) can only hold if $m < m_0$. Moreover, for each given $m < m_0$ there is n_0 with $(2t_0)^{-n_0} < 1 - (2t_0)^{-m}$, which implies that only finitely many n can fulfil (17) for $s > t_0$ together with m . Finally, for given n and m there are only finitely many 01-words v and w of length m and n , respectively. For given words v, w , the intersection point is given by a polynomial which has a finite number of solutions.

5. Another type of graph which is more likely to have large growth rate is shown in Figure 12. There is one orbit combining z and $1 - z$, defined by $g_v(z) = z, g_w(z) = 1 - z$, due to symmetry. If the lengths of v, w are m, n , respectively, the estimates (16) for the growth and (17) for nonexistence of a bounded density remain valid. This is easily shown by replacing γ^q with $\gamma^q(z) + \gamma^q(1 - z)$ in the proof of (ii). See Example 1 below, and Section 4 where we proved that such an orbit is optimal for the Fibonacci parameter. However, the above finiteness argument remains valid also for this double type of graph.
6. For Pisot parameters, there will often be more intricate network-like orbits which lead to growth rates exceeding the estimate (16). See Example 2 below and the network in Figure 13. For non-Pisot parameters, we have not found such networks. So it remains possible that beside Pisot parameters, for every $t_0 > \frac{1}{2}$ there are only finitely many numbers s for which there is an intersection point z with growth rate greater $2s$.

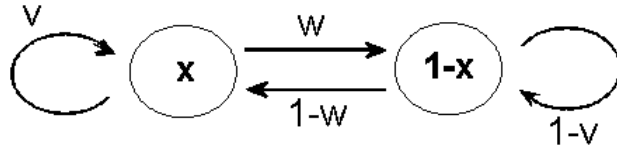


Figure 12: The two-cycle graph for a combined orbit of x and $1 - x$. Edges here stand for a whole path in Section 4, and the two paths to x may share a terminal part, as in Figure 5.

Example 1 (Perron parameter admitting a very small local dimension)

One way to find examples for Theorem 21 is to prescribe v, w and determine the corresponding s, z . To get large growth rate, we take the double type of graph in Figure 12 with $v = 10000, w = 01$. The equation $g_v(z) = z$ implies $\beta^4(\beta z + 1 - \beta) = z$ and $z = \frac{\beta^4(\beta - 1)}{\beta^5 - 1}$, and $g_w(z) = 1 - z$ yields $z = \frac{\beta}{\beta^2 + 1}$. This gives the minimal polynomial $\beta^5 - \beta^4 - \beta^2 - \beta - 1$ with Perron root $\beta \approx 1.6851$ and two complex pairs of roots of modulus 1.03 and 0.75, respectively. Thus $s = 1/\beta \approx .5934$. The point $z \approx .4389$ has growth rate $\rho \approx 1.2365$, the real solution of (16) for $m = 5, n = 2$. By Proposition 4, the local dimension of ν_s at z is $d \approx .9215$. The minimal local dimension for the Fibonacci parameter is $\frac{\log 2}{\log \tau} - \frac{1}{2} \approx 0.9404$, cf. [18, 20] and Section 4, where we have the same graph with $v = 1000, w = 01$. The Pisot parameter of the next example gives minimal local dimension 0.9380. Thus our Perron parameter has 'larger peaks' than neighboring Pisot parameters! Nevertheless, we do not expect ν_s to be singular. See Figure 3.

Example 2 (Pisot parameter with a typical network orbit)

The Pisot number $\alpha \approx 1.7049$ with minimal polynomial $\alpha^5 - \alpha^4 - \alpha^3 - 1$ was identified by Sidorov as first parameter for which a point with exactly two addresses exist (Section 9). The number $z \approx .501$ is the fixed point of g_v and g_w with $v = 10^2 10^5$ and $w = 01^2 1010^3$. Since $m = n = 9$, equation (16) gives $\sqrt[9]{2} \approx 1.08$ as lower bound for the growth rate, which is much

smaller than $\frac{2}{\alpha} \approx 1.173$. However, since we have a Pisot number we should have supercritical orbits. It turns out that the orbit of z is a network with eight branching points, and with growth factor $\rho \approx 1.2125$. This gives the local dimension 0.9380 which seems minimal for this parameter. The network is shown in Figure 13. ρ can be determined from $\det(A - I) = 0$ where A is the adjacency matrix of the network, with entries ρ^{-n} instead of 1 for edges (x, y) where $y = g_w(x)$ and w has length n . Networks without short cycles seem to be typical for Pisot numbers with high degree, where conjugates have modulus almost one. For Salem numbers of degree 4 and 6, results of Boyd indicate that the situation could be similar, see Thurston [48]. Networks can be much larger than Figure 13. However, singularities generated by complicated networks seem to have small impact on measures of neighboring parameters! This is a point which requires more study.

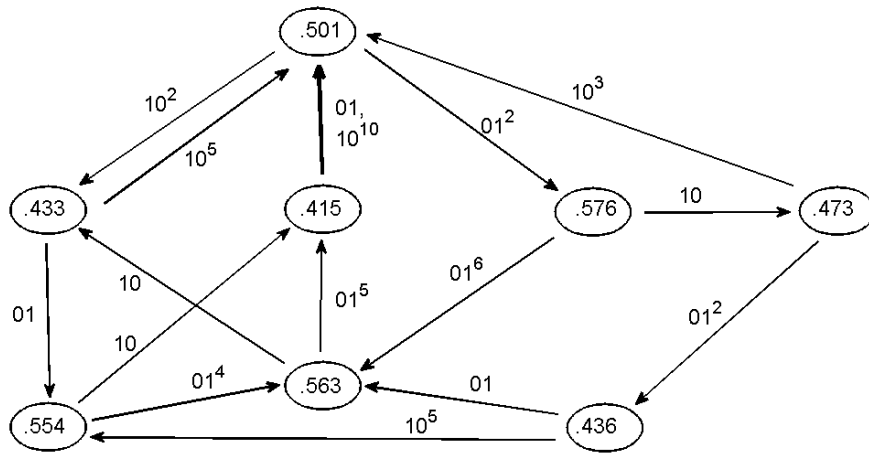


Figure 13: Network orbit with eight branch points for the Pisot parameter $\alpha \approx 1.7049$. Arrows indicate chains of maps g_0, g_1 . Two incoming chains can have a terminal part in common.

Example 3 (Generating Perron examples by screening address curves)

It is possible to determine intersection points by directly scanning periodic address curves. In Figure 14 we have chosen a window where the origin of peaks of Φ is not as obvious as for multinacci parameters, and have tried to fit the peaks by intersections of periodic address curves. This seems to work! In [8] there is a picture with less detail.

The window contains the Komornik-Loreti point, and one can distinguish the dark blue sets generated by countably many lines right of t_{KL} from the dark Cantor carpets left of t_{KL} . The Pisot parameter s_2 is also in the window, and there are many intersections of address curves at $t = s_2$ as well as near s_2 . These are mostly Pisot parameters since $1/s_2$ is a limit point of Pisot numbers (cf. Section 4). The largest peak in the window is at $(s_2, .4809)$, the intersection of curves for $b = 4/9 = .\overline{011100}$ and $c = 8/15 = .\overline{1000}$. This is an orbit of the type shown in Figure 12, with $v = 1000$ and $w = 011$. The growth rate $\rho \approx 1.221$ is obtained from $\rho^{-3} + \rho^{-4} = 1$, and the local dimension is $d \approx 0.8778$, much smaller than for the above examples and the Fibonacci number., cf. the appendix in [25].

Another Pisot parameter $s = 0.5765$ is determined by the intersection for $b = 3/7 = .\overline{011}$ and $c = 8/15 = .\overline{1000}$. This is just the intersection of a 4-cycle with a 3-cycle, and (16) gives the same growth rate as above, which leads to $d \approx 0.8963$. Figure 14 illustrates Theorem

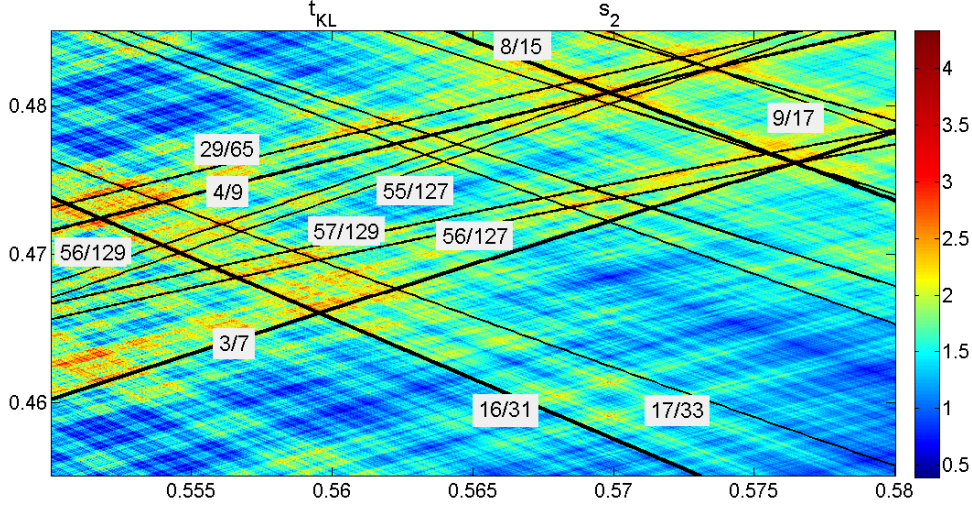


Figure 14: $\Phi(t, x)$ for $t \in [.55, .58]$, $x \in [.455, .485]$ with periodic address curves of small period. Apparently all peaks of Φ are intersections of such curves.

21(i): the address curve of $56/127 = .\overline{0111000}$ must pass through the intersection point.

Address curves in Figure 14 come in bundles: $3/7, 4/9 = 28/63, 29/65$ from the left to the upper right, $8/15$ and $9/17$ from top to right, $16/31$ and $17/33$ from upper left to lower right. Rational numbers $k/(2^p - 1)$ denote binary representations $.\overline{w_1 \dots w_p}$ of period p . A simple calculation shows that the period-doubling number $.\overline{w_1 \dots w_p (1 - w_1) \dots (1 - w_p)}$ is the rational $(k + 1)/(2^p + 1)$. The next curve of the period-doubling bundle was not drawn since it almost coincides with the second one.

These are all kneading sequences, and their canonical intersection patterns can be seen very clearly in Figures 7 and 10. Our window is in a parameter region where there are no other kneading sequences of low period. Our hypothesis is that high values of Φ can be explained by intersection of periodic address curves. To demonstrate this, we take two bundles of itineraries of period $m = 7$ which are not kneading: $55/127, 56/129$ and $56/127, 57/129$ from lower left to upper right. In [8] we proved that the intersection of $55/127$ with $16/31$ at $s \approx .5546$, $z \approx .4701$ leads to a Perron number of degree 9, and (16) with $m = 7, n = 5$ yields $\rho \geq 1.1237 > 2t$. By Proposition 4, the local dimension is $d_z(\nu_s) \leq .978$.

Now we take the intersection of $56/129$ and $16/31$ which yields $s' \approx .5540$, $z' \approx .4706$. The minimal polynomial for s' is $t^8 - t^7 + t^5 + t^4 + t^2 + t - 1$. The intersection point of any two rational functions is of course the root of a polynomial. Theorem 7 says that $\beta = 1/s'$ is a weak Perron number. It is not Pisot. We have a graph as in Figure 12. (16) applies and shows that we have the same lower bound for ρ as for s . Since $s' < s$, however, we get a slightly better estimate for local dimension: $d_{z'}(\nu_{s'}) \leq .976$. Moreover, it turns out that the orbit of z' will visit D once more than expected, and so there will be more successors of z' than estimated by (17). A numerical check showed that the large peaks of $\nu_{s'}$ at the resolution of Figure 3 can be explained by $z', 1 - z'$ and their images under maps f_v .

The intersection of $56/127$ and $16/31$ gives $s'' \approx .5566$ where $1/s''$ is a Perron number of degree 7, and (16) with $m = 7, n = 5$ again gives the same bound for the growth rate and local dimension $\leq .9841$ at $z'' \approx .4684$. Again, the orbit visits D in another point and has further branches including the fixed points of $g_{10^3 120}$ and $g_{10^2 1010}$. We have not been able

to decide whether this gives rise to a larger growth rate. A numerical approximation shows quite a number of large peaks. Finally, the intersection of $56/127$ and $17/33$ gives another Perron parameter $s^* \approx .5595$ with a graph like Figure 12 and again the same growth bound, and still supercritical: $d \leq .9928$ at $z^* \approx .4696$. .. Further Perron parameters are easy to find. Checking for supercritical growth and Pisot/non-Pisot can be left to computer. Some preliminary work was done, and many non-Pisot parameters found. Their number rapidly grows when we go with t nearer to $\frac{1}{2}$. We did not find larger network orbits for Perron parameters, however.

Example 4 (Transient growth of an orbit)

Consider the Perron number $\beta \approx 1.7924$ with minimal polynomial $x^5 - x^4 - x^3 - x^2 + x - 1$. The complex conjugates have modulus around 1.11 and 0.68. No bounded density can exist by Feng and Wang [21] since $\frac{1}{2}$ is the fixed point of g_{100010} . Since the orbit of $\frac{1}{2}$ does not contain other points of D , equation (16) gives the growth rate $\rho = \sqrt[6]{2}$ and the local dimension $d \approx .9898$ at $\frac{1}{2}$. However, there are other local dimensions and a non-trivial multifractal spectrum which will not be proved here. At a resolution of 2.5 million bins, the approximation of ν has a value 1.7 at $\frac{1}{2}$ and the maximum value 3.2 at $z \approx .46737$. It turns out that

$$g_{01110}(z) = z \text{ and } g_{1000}(z) = y \text{ with } g_{10000}(y) = y, \quad (18)$$

and the rest of the orbit apparently develops in a tree-like manner. Theorem 7 applies to z and y , and β is determined by (18) as well as by the cycles of $\frac{1}{2}$. However, the (upper) local dimensions of ν at z and at $x = g_0(y)$ must coincide although the value of x in the histogram is 1.4. The difference comes from the nonexponential growth given by the two cycles in (18) and determines a large factor C in the ansatz $\nu(U(z, r)) \approx Cr^d$ but not a large dimension d . The situation for s' and s'' in Example 3 could be similar.

A recent result of Hare, Hare and Matthews [25, Theorem 5.1] says that for Pisot parameters local dimensions of periodic orbits are dense in the set of all possible local dimensions of ν . Our figures support the conjecture that supercritical intersections of periodic address curves are present at all parameters t for which ν_t does not admit a bounded density. Although the last example indicates a difficulty, it has become clear that periodic orbits are important landmarks. Of course there are other phenomena as invariant Cantor sets and multifractal spectra which were thoroughly studied for Pisot and Salem parameters [34, 18, 19, 29, 25]. Most promising in a study of the two-variable function Φ seems parameter dependence which we did not touch here. To mention just one aspect: points with unique address outside \mathbf{D} have local dimension $1 + \frac{\log 2}{\log \beta}$ [8]. It would be interesting to know two-dimensional local dimensions at intersection points of address curves.

References

- [1] Alexander JC, Zagier D: The entropy of a certain infinitely convolved Bernoulli measure, *J. London Math. Soc.*, (2) 44, 1991, 121-134
- [2] Allouche J-P, Clarke M, Sidorov N: Periodic unique beta-expansions: the Sharkovskii ordering, *Ergodic Theory Dynam. Systems* 29 (2009), 1055-1074
- [3] Allouche J-P, Cosnard M: The Komornik-Loreti constant is transcendental, *Amer. Math. Monthly* 107 (5) (2000), 448-449

- [4] Allouche J-P, Frougny C, Hare KG: On univoque Pisot numbers, *Mathematics of Computation* 76 (259), 2007, 1639-1660
- [5] Bailey D H, Borwein J M, Calkin N J, Girgensohn R, Luke D R, Moll V H: *Experimental Mathematics in Action*, A.K. Peters 2007
- [6] Baker S: On universal and periodic β -expansions, and the Hausdorff dimension of the set of all expansions, *Acta Math. Hungar.* 142(1), 2013, 95-109
- [7] Baker S, Sidorov N: Expansions in non-integer bases: lower order revisited, *Integers* 14 (2014), Paper A57
- [8] Bandt C: The two-dimensional density of Bernoulli convolutions, arXiv 1604.00308
- [9] M.F. Barnsley, *Fractals Everywhere*, 2nd ed., Academic Press 1993.
- [10] Barnsley M., Igudesman KB: Overlapping Iterated Function Systems on a Segment, *Russian Mathematics* 56(12), 2012, 1-12
- [11] Collet P, Eckmann J P: *Iterated maps on the interval as dynamical systems*, Birkhaeuser, Basel 1980
- [12] Daróczy Z, Katai J: Univoque sequences, *Publ. Math. Debrecen* 42 (1993), 397-407
- [13] Daróczy Z, Katai J: On the structure of univoque numbers, *Publ. Math. Debrecen* 46 (1995), 385-408
- [14] de Vries M, Komornik V: Unique expansions of real numbers, *Advances in Math.* 221 (2009), 390-427
- [15] Erdős P: On a family of symmetric Bernoulli convolutions, *Amer. J. Math.* 61 (1939), 974-975
- [16] Erdős P, Joó I, Komornik V: Characterization of the unique expansions $1 = \sum_{i=1}^{\infty} q^{-n_i}$ and related problems, *Bull. Soc. math. France*, 118, 1990, 377-390
- [17] Falconer KJ: *Fractal Geometry. Mathematical Foundations and Applications*, Wiley 1990.
- [18] Feng D-J: The limited Rademacher functions and Bernoulli convolutions associated with Pisot numbers, *Advances in Math.* 195, 2005, 24-101
- [19] Feng D-J: Multifractal analysis of Bernoulli convolutions associated with Salem numbers, *Advances in Math.* 229 (2012) 3052-3077
- [20] Feng D-J, Sidorov N: Growth rate for β -expansions, *Monatsh. Math.*, 162 (1), 2011, 41-60
- [21] Feng D-J, Wang Y: Bernoulli convolutions associated with certain non-Pisot numbers, *Adv. Math.* 187 (2004), 173-194
- [22] Garsia AM: Arithmetic properties of Bernoulli convolutions, *Trans. Amer. Math. Soc.* 102, 1962, 409-432

- [23] Glendinning P, Sidorov N: Unique representations of real numbers in non-integer bases, *Math. Res. Letters* 8 (2001), 535-543.
- [24] Hare KG, Panju M: Some comments on Garsia numbers, *Math. Comp.* 82 (2013), 1197-1221
- [25] Hare K E, Hare K G and Matthews K R: Local dimensions of measures of finite type, *J. Fractal Geom.*, to appear, arXiv 1504.00510
- [26] Hutchinson J: Fractals and self-similarity, *Indiana Univ. J. Math.* 30 (1981), 713-747
- [27] Hu TY: The local dimension of the Bernoulli convolution associated with the golden numbers, *Trans. Amer. Math. Soc.* 349, 1997, 2917-2940
- [28] Igudesman KB: Dynamics of finite-multivalued transformations, *Lobachevskii Jour. of Math.* 17, 2005, 47-60
- [29] Jordan T, Shmerkin P and Solomyak B: Multifractal structure of Bernoulli convolutions, *Math. Proc. Cambridge Phil. Soc.* 151 (2011), 521-539
- [30] Kallós G: The structure of the univoque set in the big case, *Publ. Math. Debrecen* 59 (2001), 471-489
- [31] Kempton T: Counting β -expansions and the absolute continuity of Bernoulli Convolutions, *Monatsh. Math.* 171, 2013, 189-203
- [32] Kong D, Li W: Hausdorff dimension of unique beta expansions, *Nonlinearity* 28, 2015, 187-209
- [33] Komornik V, Loreti P:: Unique developments in non-integer bases, *Amer. Math. Monthly* 105 (7) (1998), 636-639
- [34] Ledrappier F, Porzio A: On the multifractal analysis of Bernoulli convolutions. I, Large deviation reults. II. Dimensions. *J Statist. Phys.* 82 (1996), 367-420
- [35] Lasota A, Mackey MC: *Fractals, Chaos and Noise*, 2nd ed., Springer, New York, 1994
- [36] Milnor J, Thurston W: On iterated maps of the interval, *Dynamical systems* (College Park, MD, 1986-87), *Lecture Notes in Math.* 1342, Springer, Berlin 1988, 465-563
- [37] Peitgen, HO, Richter PH: *The beauty of fractals: images of complex dynamical systems*, Springer, Berlin 1986
- [38] Peres Y, Solomyak B: Absolute continuity of Bernoulli convolutions, a simple proof, *Math. Research Letters* 3, no. 2, 1996, 231-239
- [39] Peres Y, Schlag W, Solomyak B: Sixty years of Bernoulli convolutions, *Fractal geometry and stochastics II (Greifswald)*, Birkhuser, 2000, 39-65
- [40] Schmidt K: On periodic expansions of Pisot numbers and Salem numbers, *The Bulletin of the London Mathematical Society* 12(4), 1980, 269-278
- [41] Shmerkin P: On the exceptional set for absolute continuity of Bernoulli convolutions, *Geom. Func. Anal.* 24, 2014, 946-958

- [42] Sidorov N: Almost every number has a continuum of β -expansions, *Amer. Math. Month.* 110(9), 2003, 838-842
- [43] Sidorov N: Universal β -expansions, *Period. Math. Hungar.* 47 (2003), 221-231
- [44] Sidorov N: Expansions in non-integer bases: lower, middle and top orders, *J. Number Theory* 129 (2009), 741-754
- [45] Sidorov N, Vershik A: Ergodic properties of Erdős measure, the entropy of the golden-shift, and related problems, *Monatshefte Math.* 126 (1998), 215-261
- [46] Solomyak B: On the random series $\sum \pm \lambda^i$ (an Erds problem) , *Annals of Math.* 142 (1995), 611-625
- [47] Solomyak B: Notes on Berboulli convolutions, In: *Fractal geometry and applications: a jubilee of Benoit Mandelbrot. Part 1*, Proc. Sympos. Pure Math. vol. 72, 207-230. Amer. Math. Soc., Providence, RI, 2004.
- [48] Thurston W P: Entropy in dimension one, *Frontiers in Complex Dynamics* (A. Bonifant, M. Lyubich, S. Sutherland, eds.), Princeton University Press 2014, 339-384
- [49] Tiozzo G: Entropy, dimension and combinatorial moduli for one-dimensional dynamical systems, PhD thesis, Harvard University, Cambridge, MA, April 2013
- [50] Varju, P: Absolute continuity of Bernoulli convolutions for algebraic parameters, arXiv:1602.00261

Christoph Bandt, Rüdiger Zeller
 Institute of Mathematics and Computer Science
 University of Greifswald, Germany
 bandt@uni-greifswald.de, rkbzeller@gmail.com